

Review

Statistical Review of Microstructure-Property Correlation of Stainless Steel: Implication for Pre- and Post-Weld Treatment

Musa Muhammed ¹, Mazli Mustapha ^{1,*}, Turnad Lenggo Ginta ¹, Abdullah Musa Ali ², Faizal Mustapha ³ and Chima Cyril Hampo ¹

¹ Department of Mechanical Engineering, Universiti Teknologi PETRONAS, Seri Iskandar 32610, Perak, Malaysia; musa_20000222@utp.edu.my (M.M.); turnad.ginta@utp.edu.my (T.L.G.); chima_19001735@utp.edu.my (C.C.H.)

² Department of Geology, Bayero University Kano (BUK), Kano 700241, Nigeria; amali.geo@buk.edu.ng

³ Department of Aerospace Engineering, UPM, Serdang 43000, Selangor, Malaysia; faizalms@upm.edu.my

* Correspondence: mazli.mustapha@utp.edu.my

Received: 15 June 2020; Accepted: 2 July 2020; Published: 10 July 2020



Abstract: For the past three centuries, there has been a very high demand for stainless steel for different applications, due to its corrosion resistance coupled with the good strength and low cost of the metal. Several welding techniques have been adopted in the fabrication of stainless steel, with the choice of welding technique hinged on the desired requirements. Advancement has been made in its dissimilar welding with other metals like aluminum, copper and titanium. While similar welding of stainless steel faces the challenge of weld metal property deterioration, dissimilar welding poses more serious challenges due to the differential in chemical composition and the thermophysical properties of the base metals. A review of the literature reveals that considerable progress has been made in the improvement of the properties of the weld joint by the application of several weld treatment processes. It was discovered that most of the researchers focused on the effect of these weld treatment processes on the properties of the weld joints, with little attempt to establish a relationship between the microstructure and properties. This review paper critically analyzed the effect of weld treatment processes on the properties of stainless steel in light of microstructure-property correlation.

Keywords: stainless steel; similar and dissimilar welding; weld treatment processes; correlation

1. Introduction

The most sought-after material, which forms the backbone of most manufacturing industries, is still stainless steel, with its combination of strength and corrosion resistance giving it an edge over the cheap and readily available carbon steel, and its low price and availability making it the preferred choice over other resistant alloys such as those of titanium. The formation of an inert film of chromium oxide on the metal surface, coupled with other alloying additions such as molybdenum, offers protection against corrosion, while nickel improves ductility and strength [1,2].

Over time, several types of stainless steel have been developed with a wide range of properties, suiting several industrial applications. The choice of stainless steel for a given application is hinged on the desired properties and service performance requirements. For instance, austenitic stainless steel finds application in biomedicine, duplex stainless steel in the automobile industry, martensitic stainless steel in turbine blades, and ferritic stainless steel in thermal power plants [3–6]. The demand for stainless steel for special applications, such as in environments where creep strength and corrosion resistance are desired, has led to the introduction of special grades of stainless steel, such as 316LN austenitic stainless steel used in international thermonuclear experimental reactors' (ITER) components,

super duplex stainless steel used in the marine industry, lean super martensitic stainless steel used in the oil and gas industry, and grade 91 ferritic stainless steel used in the petrochemical industry, among others [7–10]. Austenitic stainless steel of all the grades of stainless steel has the largest family of alloy, and has more industrial applications due to its superior service performance, and coupled with its low carbon content, which makes fabrication easy, especially by welding [11].

Welding is a permanent joining technique for creating joints using similar or dissimilar metals. A review of literature revealed that different welding techniques, such as resistant spot welding, friction welding, gas metal arc welding, laser beam welding, tungsten inert gas welding, shielded metal arc welding, electron beam welding, and plasma arc welding have been used for creating stainless joints for different applications [12–18]. The choice of welding technique depends on the size of components, quality of joints desired, precision, heat input etc. For instance, fusion welding and tungsten inert gas welding have low heat input and produce good quality joints, electron beam welding and laser beam welding have high energy input with deep weld penetration suitable for thin walled structure fabrication, and plasma arc welding has high welding speed and produces joints with high penetration to width ratio, while shielded metal arc welding is suitable for welding pipes and thick metal plates [19–25].

The welding process involves metal exposure to non-uniform heating and cooling, which ultimately results in the formation of heterogeneous microstructures, which are usually in a metastable state, alongside with residual stress [26,27]. The formation of unwanted phases, such as martensite, the sigma phase and intermetallic phases during the welding process results in the property deterioration of the material, especially at the weld joint [28–30]. The dissimilar welding of stainless steel with other metals faces additional challenges of selecting a suitable welding technique to produce good quality joints, as a result of the difference in microstructural composition and thermophysical properties [30–33].

In view of providing solutions to the aforementioned challenges, researchers have employed several weld treatment processes and hybrid welding techniques to obtain better weld properties [34–39]. Pre- and post-weld treatment processes are property modification operations carried out before and after welding processes, to improve the quality of the weld joint. Preheating, hardening and softening heat treatment processes, in-process heat treatment, shot peening, electrolytic plasma processing and plasma ion nitriding are some of the pre- and post-weld treatment processes reported by researchers in the past two decades [40–47].

In recent times, the importance of statistics as a tool for data analysis cannot be overemphasized. Correlation and regression are common statistical tools used to establish relationships between variables, with Pearson and Spearman correlation coefficient, R-squared (R^2) and adjusted R-squared (R^2 adjusted) being some of the parameters used to determine the strength of the relationship.

In the determination of linear relationships between variables, the Pearson coefficient is a preferred choice to Spearman's. Most statistical analyses are carried out using spreadsheet software packages such as IBM® SPSS® Statistics, Microsoft Excel, and Minitab, among others. In this research paper, all statistical analyses were carried out using IBM® SPSS® Statistics version 26.

Surprisingly as it may seem, despite the several studies available in literature addressing the effect of pre-and post-weld treatment on the microstructure and properties of stainless steel, only a few of them have actually established a connection or relation between themselves, despite their interdependence. For instance, the correlation between the delta ferrite composition and mechanical properties of austenitic stainless steel. Establishing this relationship would give an insight of changes in properties of stainless steel, due to changes induced in the microstructure by a weld treatment processes, thus serving as a tool for forecasting. In this review, authors analyzed the results of other researchers based on their findings on the effect of different pre-and post-weld treatments on welded stainless steel, and established a relationship between the microstructure and properties using correlation and regression.

2. Similar Welding of Stainless Steel

Most of the welded stainless steel joints in service are usually of a similar welded type of duplex, austenitic, ferritic stainless steel, or even martensitic stainless steel [48–51]. The fabrication of similar weld joints is less complicated when compared to dissimilar welding, as the properties and microstructure of the base metals are uniform. The following sections examine the different similar stainless steel weld joints in the light of effect of pre-and post-weld treatment processes.

2.1. Austenitic Stainless Steel

Austenitic stainless steel is the most frequently used grade of stainless steel for various fabrication purposes and finds application in the food industry, chemical machineries, gas turbines, nuclear power plants and surgical instruments, due to its strength, fracture toughness, weldability, formability and corrosion resistance in different environments [52–54]. With the addition of alloying elements such as molybdenum, the pitting corrosion resistance and creep strength at an elevated temperature is further increased [11]. Though several grades of austenitic stainless steel are available in service, the bulk of the ones used in manufacturing are usually the low carbon grade of 316 and 304. Their low carbon content makes them easily adopted to the welding process. In addition to the chromium and molybdenum, other alloying elements, such as nickel, manganese and silicon, are usually added in different proportions, depending on the grade of steel [55,56]. Table 1 shows the chemical composition of 316L austenitic stainless steel.

Table 1. Chemical composition of 316L austenitic stainless steel (%wt.) [56]

C	Cr	Ni	Mn	Mo	Si	P	S	Fe
0.03	16	10	2	2	1	0.045	0.03	balance

The microstructure of austenitic stainless steel largely contains the austenite phase, with a small amount of delta ferrite, and rarely some inclusions or unwanted phases [3].

The presence of delta ferrite in the microstructure in amounts up to 5% has deleterious effects on its properties when subjected to welding. Though the delta ferrite phase reduces grain boundary weakness and the tendency of hot cracking, at high temperatures, it causes embrittlement due to the formation of the sigma phase [11,57].

The precipitation of unwanted phases can be prevented using phase stabilizers of austenite phase, such as nickel, manganese, nitrogen, or those of the ferrite phase, such as chromium, molybdenum and silicon. Phase precipitation can also be prevented by controlling the cooling rate during welding, through preheating or quenching.

During cooling, austenitic stainless steel undergoes four modes of solidification containing the austenite phase, austenite-delta ferrite phase and delta ferrite phases. These phases are termed A (purely austenite phase), AF (majorly austenite with small amount of delta ferrite), FA (majorly delta ferrite and small amount of austenite) and F (purely delta ferrite phase) [58]. The application of proper pre- and post-weld treatment have also been reported to eliminate unwanted phases and homogenize the microstructure of austenitic stainless steel.

Nam et al. [57] investigated the effects of annealing temperature and holding time on the properties of austenitic stainless steel. They reported that the hardness and tensile strength of the weld metal decreased with increasing annealing temperature as a result of the formation of coarse austenite grains and release of residual stresses. The precipitation of carbides at the temperature range of 650–850 °C was also observed, but dissolved at high annealing temperatures. Hamada et al. [28] and Tseng et al. [59] also reported carbide precipitation in austenitic stainless steel, with post-weld heat treatment in that temperature range. The precipitation of intermetallic carbides is attributed to the instability of ferrite phase stabilizers in that temperature range, as reported by Sahlaoui and Sidhom [60] and Sahlaoui et al. [61] The fluctuation observed in the elongation is as a result of the fluctuation in

carbide precipitation with an annealing temperature. The fracture toughness was found to decrease between the temperature range of 650–850 °C, as also reported by Kozuh et al. [11], who opined that the reason for the reduction is the precipitation of the sigma phase.

A common phenomenon which occurs during the welding of the thin walled structure using electron beam welding is the buckling effect, which occurs due to thermal tensioning of the weld metal, as a result of temperature differences between the weld metal and the adjacent metal [62,63]. The application of the heat treatment, as reported by some researchers in preventing buckling, is not usually considered, because of its time consuming nature and the inability to control the precipitation of unwanted phases [64,65]. Zhang et al. investigated the effect of multi-beam preheating in buckling effect reduction in austenitic stainless steel, and concluded that multi-beam preheating reduces buckling distortion by 80%. The reduction of the buckling effect is as a result of the thermal stress relieving process induced by the preheating [66].

In addition to the hardness reduction and improvement in mechanical properties, post-weld heat treatments are used as stress relieving mechanisms. Post-weld cool treatment is a form of post-weld treatment which is based on the principle of reverting the tensile stresses set up during the welding process to compressive stress, by making the temperature of the weld metal lower than of the adjacent metal. This is achieved by using a cooling fluid, such as water, supplied at a constant velocity for a given time period. Jia et al. [67] investigated the effect of preheating and post-weld cool treatment on residual stress reduction. In their research, post-weld cool treatment was applied to austenitic stainless steel, over a cooling range of 1.5–2 times the weld width.

They concluded that post-weld cool treatment reduces longitudinal residual stresses while preheating reduces both longitudinal and transverse residual stresses. The residual stresses were also found to decrease with increasing cooling range with cooling time having no significant effect.

An enhanced form of low carbon 316 austenitic stainless steel finds application in the fabrication of International Thermonuclear Experimental Reactor (ITER) components. Xin et al. [68], studied the effect of different post-weld age treatment on the properties of this grade of steel. The results of their findings revealed that increasing the ageing temperature coarsened the cells and dendrites with the occurrence sub-grain boundaries at high temperatures. They also reported no significant changes in the tensile strength and yield strength as a result of microstructural stabilization by nitrogen and manganese which are austenite phase stabilizers. The increment observed in elongation and impact energy is due to the release of residual stresses and precipitation of sigma phase respectively [69].

In addition to residual stress relief, applying a brief post-weld treatment to austenitic stainless steel improves corrosion resistance. In view of this, Zareie Rajani et al. [1] investigated the effect of controlled preheating on the corrosion properties of austenitic stainless steel. They observed an improved corrosion resistance for samples with controlled preheating. The increase in corrosion resistance was attributed to reduction in amount of delta ferrite, due to the reduction in cooling rate, giving room for transformation. This is accompanied by a reduction in austenite-delta ferrite interfaces, which are pitting corrosion sites.

Consequently, despite the deleterious effects of delta ferrite and carbide precipitates in the austenitic stainless steel microstructure, they also confer certain desired properties. For instance, delta ferrite transforms to sigma phase at elevated temperatures, which improves grain boundary strengthening and reduces the tendency of cracking at elevated temperatures. The prevention of carbide precipitation and the elimination of delta ferrite can be achieved by introducing alloying additions or controlling the cooling rate by applying weld treatment processes. Aside carbide precipitation prevention, controlling the cooling rate of austenitic stainless steel reduces residual stresses, improves corrosion resistance, and reduces buckling distortion.

From the forging, it is clear that the properties of austenitic stainless steel weld are highly dependent on the delta ferrite composition and precipitation of carbides. Table 2 shows the delta ferrite composition of austenitic stainless steel at different holding times.

Table 2. Delta ferrite composition (%) of austenitic stainless steel at different temperatures and holding times [57].

Temperature (°C)	Holding Time (Hours)			
	0.5	1	2	4
850	7.5	7.4	7.2	6.8
900	7.0	6.5	6.1	5.6
950	6.5	5.6	4.4	4.2
1000	6.0	4.6	3.7	2.8

A bivariate correlation analysis of the data in Table 2 revealed that a perfect negative correlation with Pearson correlation coefficient in the range of -0.925 to -1 exists between delta ferrite composition and the annealing holding time, as can be seen in Table 3. A similar negative correlation was obtained between the delta ferrite composition and annealing temperature, as can be seen in Table 4.

Table 3. Correlation between annealing holding time and delta ferrite composition at different temperatures.

Annealing Temperature (°C)	Pearson Correlation Coefficient
850	-1
900	-0.96
950	-0.871
1000	-0.925

Table 4. Correlation between annealing temperature and delta ferrite composition at different holding times.

Annealing Holding Time (Hours)	Pearson Correlation Coefficient
0.5	-1
1	-1
2	-0.993
4	-1

This implies that, at low temperatures in the range of 800 – 850 °C and a holding time of less than an hour, there is a tendency to have high delta ferrite composition as vice versa. The reduction in delta ferrite composition at high annealing temperatures and long holding times is an indication of delta ferrite transformation to the sigma phase. Similar correlation between annealing temperature and delta ferrite composition was obtained from the analysis of the data in Table 5.

Table 5. Delta ferrite composition and mechanical properties of austenitic stainless steel at different annealing temperatures in the range of 600 – 900 °C [11].

Mechanical Property	Annealing Temperature (°C)			
	600	700	800	900
Delta Ferrite Composition (%)	11.7	8.0	0.9	0.5
Hardness (HV)	240.9	233.7	241.5	232.3
Tensile Strength (MPa)	819.3	835	836	791

In order to ascertain the relationship between delta ferrite composition and the mechanical properties of austenitic stainless steel, a bivariate correlation analysis was carried out using the data

in Tables 5 and 6. The results revealed that there is a high positive correlation between delta ferrite composition and tensile strength, and the strength of correlation reduced when annealing was carried out at a lower temperature range, as can be seen in Tables 7 and 8. A weak positive correlation was obtained for the hardness, while hardness and tensile strength were found to be moderately positively correlated. This corroborates the fact that an increase in hardness implies a corresponding increase in strength of austenitic stainless steel weld joints.

Table 6. Delta ferrite composition and mechanical properties of austenitic stainless steel at different annealing temperatures in the range of 650–1050 °C [57].

	Temperature (°C)		
Mechanical Property	650	850	1050
Delta Ferrite Composition (%)	6.5	7.5	5.5
Hardness (HV)	200	173	168
Tensile Strength (MPa)	590	590	540

Table 7. Pearson correlation coefficient between delta ferrite composition and mechanical properties of austenitic stainless steel at high annealing temperatures (650–1050 °C).

	Hardness (HV)	Tensile Strength (MPa)
Delta Ferrite Composition (%)	0.145	0.866
Tensile Strength (MPa)	0.620	

Table 8. Pearson correlation coefficient between delta ferrite composition and mechanical properties of austenitic stainless steel at low annealing temperature (600–900 °C).

	Hardness (HV)	Tensile Strength (MPa)
Delta Ferrite Composition (%)	0.243	0.303
Tensile Strength (MPa)	0.525	

A relationship between delta ferrite composition and the corrosion resistance of austenitic stainless steel was obtained by carrying out a bivariate analysis using the data in Table 9. The results in Table 10 reveal that delta ferrite composition is perfectly positively correlated with corrosion current density and perfectly negatively correlated with preheating temperature. This implies that better corrosion resistance is obtained at low delta ferrite compositions and high preheating temperatures, and reaffirms that preheating improves the corrosion resistance of austenitic stainless steel.

Table 9. Corrosion current density and delta ferrite composition of austenitic stainless steel at different preheating temperatures [1].

Preheating Temperature (°C)	Delta Ferrite Composition (%)	Corrosion Current Density ($\mu\text{A}/\text{cm}^2$)
24	12.3	6.92
450	9.2	5.25
650	6.4	3.89

Table 10. Pearson correlation coefficient between delta ferrite composition, corrosion current density and preheating temperature.

	Corrosion Current Density ($\mu\text{A}/\text{cm}^2$)	Preheating Temperature (°C)
Delta Ferrite Composition (%)	1.00	−0.985

Mathematical models for the properties of austenitic stainless steel in terms of delta ferrite composition were obtained by regression analysis using the data in Tables 5 and 9. Table 11 gives the model summary, and Figure 1a–c shows the normal probability plot. R^2 and Adjusted R^2 given in the table are estimators which give an insight into the predictive power of the model. As a rule of thumb, the closer the values of these estimators are to unity, the more accurate the model becomes.

Table 11. Model summary of the properties of austenitic stainless steel in terms of delta ferrite composition.

Property	Model	R^2	Adjusted R^2
Hardness (HV)	$332.912 - 0.112T - 2.294F$	0.835	0.504
Tensile Strength (MPa)	$1184.752 - 0.427T - 8.422F$	0.686	0.058
Corrosion Current Density ($\mu\text{A}/\text{cm}^2$)	$0.573 + 0.514F$	0.999	0.998

Note that F in Table 11 denotes delta ferrite composition (%), while T denotes annealing temperature ($^{\circ}\text{C}$).

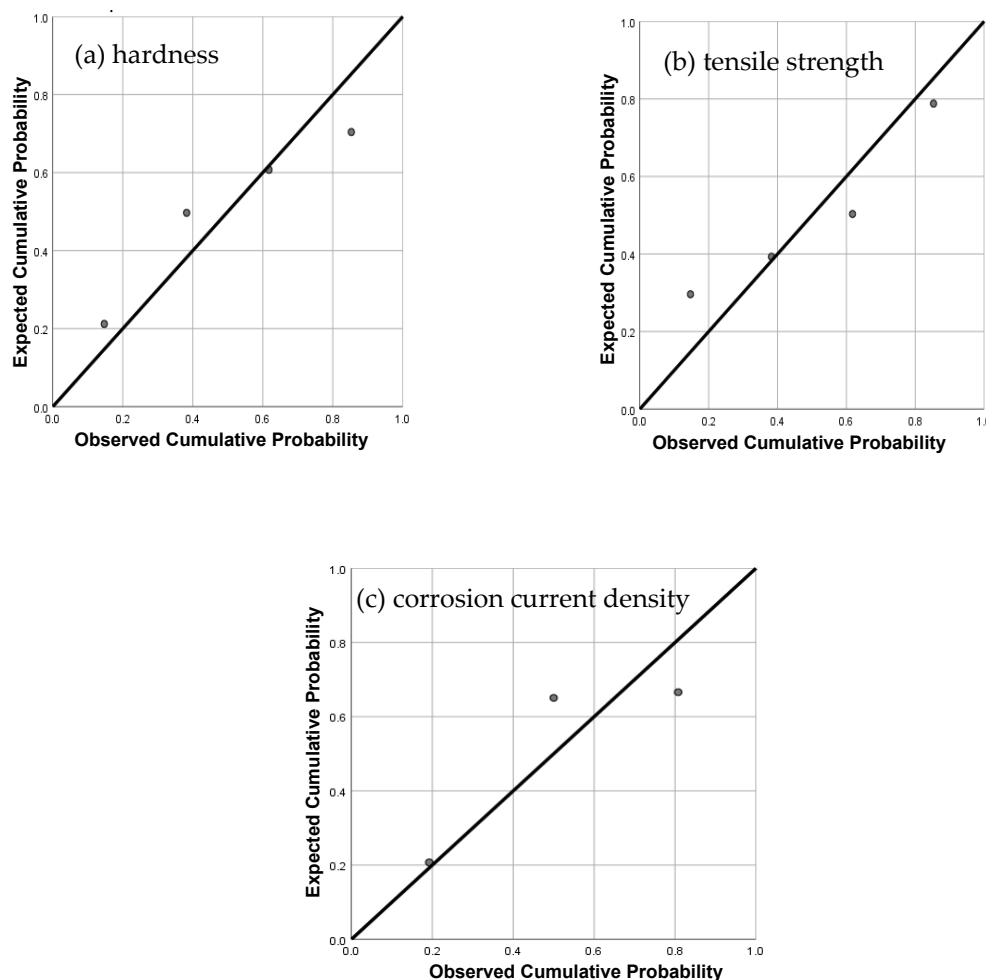


Figure 1. Normal probability plot of properties of austenitic stainless steel: (a) hardness; (b) tensile strength; (c) corrosion current density.

2.2. Duplex Stainless Steel

Duplex stainless steel, also known as dual phase stainless steel, finds application in the automobile industry, petrochemical industry, paper industry, and marine applications, among others. The wide range of applications of duplex stainless steel is as a result of its toughness, yield strength, work

hardening rate, formability, corrosion resistance, light weight and crash worthiness [4,24,59,70–79]. Special industrial requirements, such as strength and corrosion resistance at elevated temperatures, led to the development of higher grades of duplex stainless steel, which are used in boilers, pressurized reversed osmosis plants, firefighting systems and heat exchangers [70,80].

The desired properties of duplex stainless steel are as a result of the equilibrium between hard ferrite and soft austenite, in addition to other alloying elements such as chromium, molybdenum, vanadium and nitrogen [81,82], as researchers have reported that optimum properties have been obtained in duplex stainless steels when the ratio of ferrite to austenite is approximately 1 [83–87].

The microstructure of duplex stainless steel comprises dispersed austenite and ferrite phases in approximately equal amounts, and other alloying elements depending on the grade of duplex stainless steel [81,82,88–92]. Table 12 shows the chemical composition of duplex stainless steel.

Table 12. Chemical composition of DP 980 dual phase stainless steel [91].

C	Cr	Mn	Si	S	P	Al	Cu	Fe
0.13	0.2	1.326	0.13	0.014	0.004	0.036	0.196	balance

The low carbon content of duplex stainless steel increases their weldability. A number of welding techniques have been reported to have been used to fabricate different grades of duplex stainless steel [51,93–96]. Some of the challenges encountered include the hardness of the fusion zone, the formation of shrinkage voids, weld failure, mainly in the interfacial mode, and general property deterioration across welded joints [29,97–99]. Weld property deterioration in duplex stainless steel is attributed to the upset in equilibrium between the austenite and ferrite phases. Another contributing factor is the formation of secondary unwanted phases, such as sigma, intermetallics and chi phases during the welding process, as the ferritization (increase in ferrite content) of duplex stainless steel in the weld metal leads to the formation of intermetallics and martensite upon solidification [90,100–102].

The solidification transformation of ferrite to austenite in duplex stainless steel is usually in three forms; grain boundary austenite (GBA), Widmanstätten austenite (WA) and intergranular austenite (IGA), with GBA and WA being the most common ones, as their formation at high temperatures requires a very low driving force [82,103–105].

In the desire to improve the properties of welded duplex stainless steel, researchers have applied several pre- and post-weld treatments, ranging from in-process and post-weld tempering, to brief annealing post-weld treatment, to shot peening, to plasma ion nitriding, to laser continuous heat treatment.

Nikoosohbat et al. [91] investigated the effect of an in-process tempering on the properties of duplex stainless steel. An in-process tempering is the application of post-weld tempering current pulse to the weld metal and the magnitude is dependent on the metal thickness, weld composition and desired properties. Their findings revealed that the hardness of the weld metal reduced with increasing tempering current cycle due to the tempering of the hard martensite. The tensile shear strength and peak load of the samples which failed in an interfacial failure mode were found to be a function of the hardness as samples without in process tempering possessed the highest tensile shear strength. In other words, there is a correlation between the hardness and strength of the weld metal.

The effect of post-weld tempering on the properties of duplex stainless steel was studied by Luo et al. [99] The result of their experiment revealed that the ferritization of the weld metal, alongside the precipitation of secondary austenite phase and sigma phases, occurs during the welding process. Upon post-weld tempering, all the phases increased in intensity, exhibiting a segregational phenomenon, leading to an overall reduction in hardness. This led to a conclusion that, despite hardness reduction by post-weld tempering, it poses detrimental effects on the mechanical properties of duplex steel, as it precipitates deleterious secondary phases.

Brief annealing post-weld treatment is one of the processes adopted to prevent the precipitation of deleterious secondary phases and unwanted transformation in the microstructure of duplex stainless

steel. In this regard, Zhang et al. [90] investigated the effect of brief annealing post-weld treatment on the properties of duplex stainless steel. As expected, they reported the presence of ferrite phase stabilizers such as chromium and molybdenum in the ferrite phase, as well as austenite phase stabilizers such as nickel in the austenite phase. The hardness of the weld metal was found to increase at temperatures above the equilibrium temperature as a result of excessive ferritization, coupled with the precipitation of the solid solutions of chromium and molybdenum, which was accompanied by a reduction in impact energy. The improvement in impact energy observed at low annealing temperatures is a result of reduction in residual stress coupled with the balanced phase composition.

Some researchers have also reported that brief annealing post-weld treatment affects the corrosion properties of duplex stainless steel [106,107]. In view of this, Yang et al. [92] investigated the effect of annealing temperature and brief holding time on the properties of duplex stainless steel. They observed an overall reduction in the corrosion resistance of the weld metal, which was attributed to the excessive ferritization of the weld joint, which eventually led to the precipitation of nitrides and the disruption of the ferrite-austenite equilibrium. Nitride precipitation in duplex stainless steel reduces corrosion resistance by enhancing the critical current density and passivation potential, as reported by Parren et al. [108] The reduction in corrosion resistance was characterized by selective attack of the ferrite phase in the critical pitting test (CPT) analysis. Subsequently, upon application of the brief annealing post-weld treatment, the corrosion resistance was improved with increasing holding time and temperature. This was characterized by deferritization of the weld joint and increase in stabilizers of the austenite phase to obtain a microstructure almost similar to that of the base metal. They concluded that the pitting resistance equivalent number (PREN) of duplex stainless steel is a function of the PREN of the weaker phase.

Varying the heat input during the welding process is a form of the weld treatment process applied to duplex stainless steel, as reported by some researchers. Heat input variation can be achieved by altering the welding speed, the voltage or current or welding time depending on the welding technique adopted. Slow welding speed, high welding current and long welding time is an indication of high energy input as vice versa [109]. The effect of welding speed on briefly annealed duplex stainless steel was investigated by Saravanan et al. [110] The results of their study revealed that the application of post-weld annealing treatment increases the austenite phase composition, which is in line with the findings of Pramanik et al. [111] The increase in hardness observed with low welding speed is attributed to the ferritization of the weld joint, due to high energy input and increase in residual stresses. It may also be as a result of the formation of finer grains, or the precipitation of phase stabilizers such as nitrogen, chromium, silicon and manganese in the weld zone, as reported by Saravanan et al. [112] They concluded that the improvement in corrosion resistance and the reduction in hardness of duplex stainless steel is as a result of reduction in weld zone ferritization and reduction in residual stresses.

Liu et al. [89] studied the effect of continuous laser heating on the properties of duplex stainless steel. The result of their findings revealed that laser heating improved the mechanical properties of duplex stainless steel, by reducing the ferritization of the weld zone and increasing the formation of secondary austenite of the Widmanstätten type.

The corrosion tests revealed the selective attack of the ferrite phase of the weld metal, and an improvement in corrosion resistance was achieved by increasing laser heating energy, which eliminated nitrides from the ferrite zone, coupled with the ferrite transformation to Widmanstätten austenite.

Shot peening and nitriding are surface modification processing technologies which can be applied to welded joints to reduce crack propagation, residual stresses, surface hardness and increase wear resistance. Shot peening is a coldworking non-destructive surface treatment process which is applied to the top, middle or bottom part of a material, leading to the generation of compressive stresses which deforms the material plastically, resulting in high impact strength [113–115]. The effect of shot peening and nitriding on the properties of duplex stainless steel was investigated by Selvabharathi et al. [88] They observed that shot peening created defects on the metal surface which were occupied by nitrogen upon nitriding, and reformed the grain boundaries to produce micro twins. The formation of micro

twins in duplex stainless steel has been reported to provide strain energy that transforms austenite to martensite [115]. Despite the precipitation of the S phase during the welding process, the increased hardness of the nitrided weld metal is attributed to the micro twin grain boundaries and the precipitated martensite. Though the precipitation of the S phase has a detrimental effect on the hardness of duplex stainless steel, it has also been found to prevent the formation of chromium nitride, which implies an increase in corrosion resistance [116]. They concluded that overall improvement in the tensile strength of the shot peened nitrided duplex stainless steel was attributed to the fine martensite grains, reduction in residual stresses and increased twin grain boundaries.

Summarily, it can be said that optimum properties in duplex stainless steel are obtained when the austenite and ferrite phase are in equilibrium and their quotient is approximately 1. Welding upsets this equilibrium, and in turn, leads to property deterioration, by setting up residual stresses and precipitating unwanted secondary phases through ferritization. In spite of the deleterious effect of the S phase and delta ferrite on the properties of duplex stainless steel, they have been found to improve corrosion resistance. The improvement in properties of welded duplex stainless steel joints through weld treatment processes is achieved by deferritization, the release of residual stresses and martensite tempering.

It is apparent that the properties of duplex stainless steel are a function of the ferrite phase and phase stabilizers, such as chromium, nickel, molybdenum and manganese; hence, the need to establish a correlation between them. Tables 13 and 14 show the ferrite phase composition, properties and composition of phase stabilizers at different temperatures of duplex stainless steel. The chromium and molybdenum are those of the ferrite phase, while the nickel and manganese are those of the austenite phase, since the former are ferrite phase stabilizers, and the latter are austenite phase stabilizers.

Table 13. Mechanical properties, ferrite and phase stabilizers' composition of duplex stainless steel at different temperatures [90].

Temperature (°C)	1020	1050	1080	1100
Ferrite Content (%)	51	50.5	52.5	54
Hardness (HV)	300	287	286	298
Impact Toughness (J)	70.1	84.1	90.8	79.5
Cr (Wt %)	26.2	26.3	26.0	25.8
Mo (Wt %)	4.4	4.6	4.4	4.3
Ni (Wt %)	7.8	8.0	8.2	8.4
Mn (Wt %)	0.81	0.82	0.83	0.83

Table 14. Properties, ferrite and phase stabilizers composition of duplex stainless steel at different heat inputs [89].

Heat Input (kW)	0	4	6	8
Ferrite Content (%)	70	62	59	64
Ultimate Tensile Strength (MPa)	780	790	800	780
Corrosion Current Density ($\mu\text{A}/\text{cm}^2$)	62.03	54.77	69.28	28.08
Cr (%)	22.34	22.89	23.01	22.48
Mo (%)	0.36	0.38	0.39	0.36
Ni (%)	1.18	1.39	1.30	1.25
Mn (%)	1.52	1.59	1.58	1.55

The results from the correlation analysis of the data in Table 13 revealed that a weak positive correlation exists between the ferrite content and hardness, while a moderate negative correlation

exists between the impact toughness and ferrite content, as can be seen in Table 15. This implies that increasing the ferrite content is likely to be accompanied by low impact toughness and increased hardness, which is an indication that ferritization in duplex stainless steel has detrimental effects on the mechanical properties.

Table 15. Pearson correlation coefficient between ferrite content and properties of duplex stainless steel.

	Hardness (HV)	Impact Toughness (J)	Ultimate Tensile Strength (MPa)	Corrosion Current Density ($\mu\text{A}/\text{cm}^2$)
Ferrite Content (%)	0.246	−0.426	−0.843	−0.121

The ferrite composition was found to be strongly negatively correlated with ultimate tensile strength, and slightly negatively correlated with corrosion current density, as can be seen in Table 15. This implies that increasing ferrite composition in duplex stainless steel is accompanied by a corresponding decrease in ultimate tensile strength, and less likely with an increased corrosion resistance. This verifies that increasing the ferrite phase leads to a deterioration in the mechanical and corrosion properties of duplex stainless steel.

The relationship between phase stabilizers and ultimate tensile strength was also obtained by carrying out a similar bivariate correlation analysis using the data in Table 14. The results, as can be seen in Table 16, reveal that a perfect correlation exists between ferrite phase stabilizers (Cr and Mo) and ultimate tensile strength, while a moderate to strong correlation was obtained with austenite phase stabilizers (Ni and Mn). The increase in ferrite phase stabilizers content denotes an increase in ferritization, which also implies an increase in strength, and thus validates that a significant correlation exists between the hardness and strength of duplex stainless steel.

Table 16. Pearson correlation coefficient between phase stabilizers and ultimate tensile strength of duplex stainless steel.

	Cr (%)	Mo (%)	Ni (%)	Mn (%)
Ultimate Tensile Strength (MPa)	0.944	0.986	0.591	0.771

Mathematical models were also obtained for the properties of duplex stainless steel in terms of ferrite composition, using the data in Tables 13 and 14. Table 17 and Figure 2a–d give a summary of the models and the normal distribution plots, respectively.

Table 17. Model summary for properties of duplex stainless steel in terms of ferrite phase composition.

Property	Model	R ²	Adjusted R ²
Hardness (HV)	$254.924 + 8.272F - 3.69T$	0.809	0.428
Impact Toughness (J)	$5490.072 + 232.666F - 16.329T$	0.998	0.993
Ultimate Tensile Strength (MPa)	$968.706 - 2.710F - 1.879H$	0.938	0.813
Corrosion Current Density ($\mu\text{A}/\text{cm}^2$)	$337.778 - 3.979F - 6.789H$	0.855	0.564

In Table 17, F denotes the percentage ferrite phase composition and T is the post-weld heat treatment temperature, while H is the heat input.

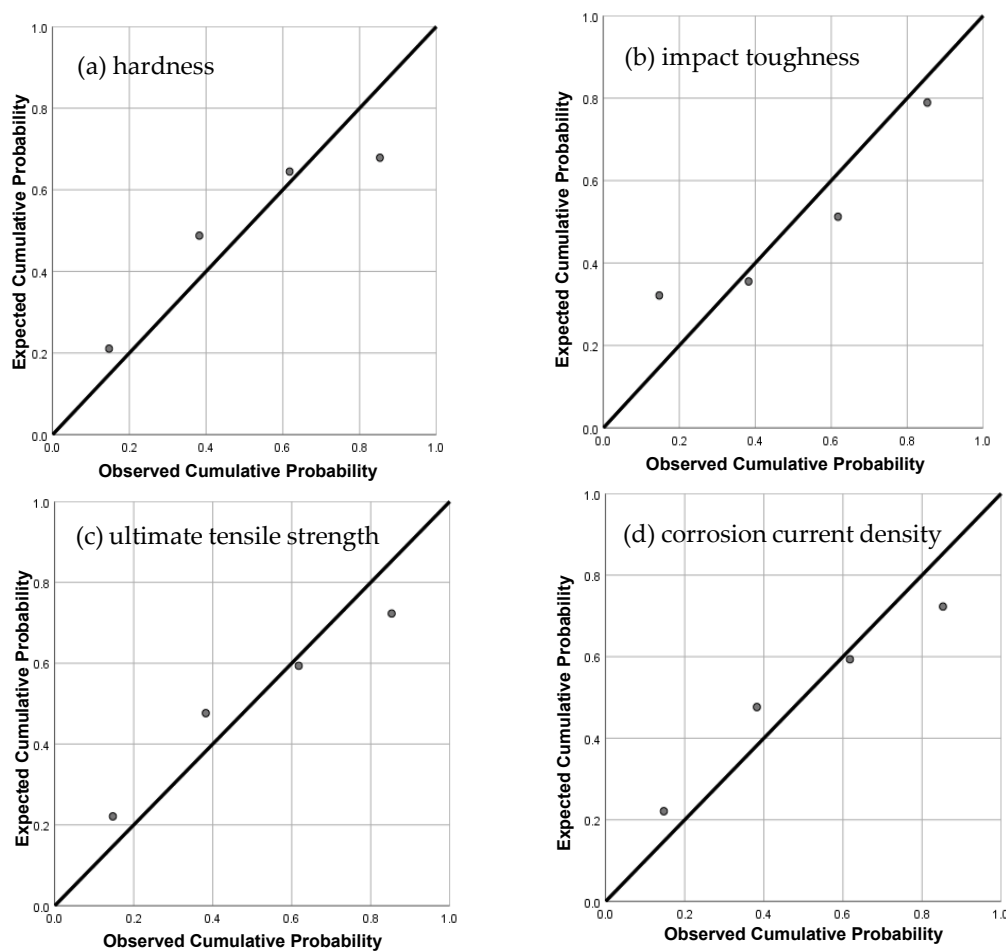


Figure 2. Normal probability plot of properties of duplex stainless steel: (a) hardness; (b) impact toughness; (c) ultimate tensile strength; (d) corrosion current density.

2.3. Martensitic Stainless Steel

Martensitic stainless steel finds application in nuclear power plants, the oil and gas industry, hydraulic turbines, pumps, shafts, surgical tools and bearings, due to its favorable mechanical properties, corrosion resistance, ease of heat treatment and weldability [5]. The need to improve the corrosion resistance, hardness, weldability and creep strength of martensitic steels for special industrial applications led to the development of higher grades of martensitic steel, such as super martensitic stainless steel (SMSS), lean super martensitic stainless steel (LSMSS), reduced activated ferritic martensitic (RAFM) stainless steel, China low activation martensitic (CLAM) stainless steel and maraging stainless steel [117]. In these grades of martensitic stainless steel, there is a reduction in the carbon composition to improve weldability, an increase in nickel and molybdenum content to stabilize martensite microstructure, and an improvement in the corrosion resistance with other alloying additions, such as titanium, vanadium and copper, to confer other properties [118,119].

The microstructure of martensitic stainless steel comprises martensite, austenite and ferrite phases, with the primary phase being martensite [120]. Table 18 shows the chemical composition (%weight) of AISI 420 martensitic steel.

Table 18. Chemical composition (%weight) of AISI 420 martensitic stainless steel [121].

C	Cr	Mo	Mn	Si	P	S	Ni	Al	Fe
0.351	13.71	0.084	0.548	0.562	0.024	0.009	<0.3	<0.02	balance

The low carbon content of martensitic stainless steel improves their weldability, but they face a major setback of poor weld properties, due to the presence of brittle martensite and delta ferrite at the weld joint. The presence of martensite leads to cold cracking and eventually material failure, while delta ferrite deteriorates the mechanical properties of martensitic steel [122–126].

The improvement of poor weld properties in martensitic stainless steel can be achieved by refining the martensite grains and the precipitation of secondary phases along grain boundaries, which serve to resist dislocation movement, thus improving strength. This can be achieved by the application weld heat treatment processes; mainly the preheating, tempering, normalizing, aging and solution treatment [127,128].

The effect of preheating and post-weld tempering on the properties of martensitic stainless steel was investigated by Köse and Kaçar [121]. The result of their research revealed that the weld metal contained a large amount of martensite and a small amount of delta ferrite. A similar result was reported by Baghjari and Akbari Mousavi [124] and Berretta et al. [129] The hardness of the weld metal was found to be improved by preheating and post-weld tempering, due to the reduction in cooling rate by preheating, which activated the martensite–ferrite transformation and coupled with the precipitation of fine carbides. The reduction of hardness of the weld metal in martensitic weld joints due to fine carbide precipitation has also been reported by other researchers [130,131]. Reduction in hardness implies an increase in toughness and formability, and it is usually accompanied by reduction in chromium content, which implies poor corrosion properties.

Post-weld tempering temperature has also been reported to affect the tensile strength of martensitic stainless steel. Muthusamy et al. [120] investigated the effect of post-weld tempering temperature and heat input on the properties of martensitic stainless steel. They reported that increasing heat input increases the toughness and hardness of the weld metal, while the tensile strength was found to decrease with both increasing heat input and tempering temperature. The increase in toughness and hardness of the weld metal and the reduction in tensile strength was attributed to the increase in delta ferrite composition, with increasing tempering temperature and heat input.

The effect of tempering holding time on the properties of martensitic stainless steel was studied by Tavares et al. [132] In their experiment, a post-weld tempering temperature of 650 °C was applied, while varying the holding time between 15–60 min. They found out that the hardness, toughness and elongation of the weld metal reduced with holding time as a result of martensite tempering, and coupled with the precipitation of intermetallic phases containing molybdenum, while no significant effect was observed in the tensile properties.

The level of retained austenite phase in martensitic stainless steel determines its mechanical and corrosion properties. With the objective of improving the mechanical properties of martensitic stainless steel by increasing the level of retained austenite, Zappa et al. [133] investigated the combined effect of double tempering and solution treatment on preheated martensitic stainless steel. They discovered that the level of retained austenite increased from 14% to 42% after the second tempering. The application of first tempering reduced the hardness and tensile properties, while toughness and elongation were improved. The application of the double tempering was found not to have a significant improvement in mechanical properties, despite the increase in retained austenite content.

Kumar et al. [134] investigated the effect of normalizing post-weld treatment on the properties of martensitic steel. They found out that the hardness and ultimate tensile strength of martensitic steel reduced with increasing preheat temperature, and increased with the normalizing temperature. A reverse trend was reported for the impact energy and ductility. The reduction in hardness and ultimate tensile strength, which was accompanied by an increase in ductility and impact energy with increasing preheat temperature, was as a result of the reduction in cooling rate, which coarsened the microstructure. Meanwhile, increasing normalizing temperature on the other hand increased the cooling rate and refined the microstructure.

Reduced activated ferritic martensitic (RAFM) stainless steel and China low activation martensitic (CLAM) stainless steel are two grades of martensitic stainless steel that have applications in ITER

components due to their high creep strength. Manugula et al. [135] investigated the effect of post-weld direct tempering (PWDT) and post-weld normalization tempering (PWNT) on the properties of RAFM stainless steel. The results of their experiments revealed that both PWDT and PWNT reduce the hardness of the weld metal, with PWNT providing a greater reduction. Hardness reduction by PWDT was as a result of martensite tempering, loss of solid solution strengthening and the elimination of dislocation associated with the transformation of martensite. Meanwhile, a reduction in hardness by PWNT was solely as result of martensite tempering. As for the impact energy, PWNT increased the impact energy, while PWDT brought about its reduction. The poor impact energy offered by PWDT was as a result of high carbon martensite and the presence of delta ferrite, while the presence of tempered martensite coupled with delta ferrite elimination improved the impact energy during PWNT. The ultimate tensile strength followed the same trend, while the elongation was found to be higher for the sample with PWDT.

A similar study on the effect of PWNT time on the properties of CLAM stainless steel was investigated by Li et al. [136] The hardness of the weld metal was found to decrease with increasing tempering time, due to the sufficient time available for martensite transformation. They also reported a decrease in heat shock resistance and ultimate tensile strength with increasing tempering time, while the elongation and impact energy followed a reverse trend. The presence of lath martensite in the weld metal accounted for its superior thermal shock resistance. The authors recommended PWNT of 30 min for better property combination for applications involving thermal shock resistance.

Maraging stainless steel is a low carbon martensitic steel produced by age hardening, possessing ultra-high strength, fracture toughness, excellent machining properties and weldability. Its favorable properties are the reasons behind its adoption as a structural element in the aviation and space industry, and in defense and power applications.

Fe-Ni and Fe-Cr-Ni are two major types of maraging steel available. However, in recent terms, a lot of alloying modifications have been made for improved performance [137,138]. Microstructural changes or property modification in maraging steel are achieved by solution annealing and precipitation hardening.

An et al. [139] investigated the effect of ageing heat treatment on the properties of Fe-Cr-Ni type maraging stainless steel. The result of their findings revealed that ageing produces a homogeneous microstructure with less alloying elements, and the microstructural homogeneity was found to have a positive correlation with ageing temperature. Hardness variation observed across the weld metal was attributed to the microstructural evolution mechanisms resulting from the different alloying elements present in martensite.

To sum up, the presence of martensite and delta ferrite in the weld joints of martensitic stainless steels has detrimental effects on their properties; predominantly hardness and ultimate tensile strength. However, for applications where resistance to thermal shock is desired, martensite phase is desired. The application of weld treatment processes such as preheating, normalizing, tempering and ageing improves the mechanical properties. Preheating and increasing post-weld treatment time reduces hardness and tensile strength, by reducing the cooling rate, martensite tempering and precipitation of intermetallic phases. A reduction in hardness is also achieved by normalizing and tempering, but normalizing confers greater strength than the latter. Increasing the ageing temperature, on the other hand, homogenizes the microstructure, and the extent of homogeneity is strongly correlated with the temperature.

Subsequently, increasing the ferrite content in martensitic steel implies a reduction in the martensite phase. Thus, controlling the ferrite content is another way of modifying the properties of martensitic steel. Table 19 shows the mechanical properties of martensitic stainless steel at different ferrite composition. Establishing a correlation relationship between these properties will reveal how changes in one property affect the other. The results of the correlation are given in Table 20.

Table 19. Mechanical properties of martensitic stainless steel at different ferrite compositions [120].

Ferrite Content (%)	37	41.49	43
Ultimate Tensile Strength (MPa)	518	517	497
Hardness (HV)	271	279	284
Impact Toughness (J)	141	148	164

Table 20. Pearson correlation coefficient between ferrite content and mechanical properties of martensitic stainless steel.

	Hardness (HV)	Impact Toughness (J)	Ultimate Tensile Strength (MPa)
Ferrite Content (%)	0.989	0.877	−0.724
Hardness (HV)			−0.817

The bivariate analysis revealed that the ferrite content is perfectly positively correlated with hardness and impact toughness. This implies that increasing the ferrite content of martensitic steel is likely to produce a corresponding increase in the hardness and impact toughness. A perfect negative correlation was also observed between the hardness and strength of martensitic stainless steel. This justifies the case of normalizing, as it reduces the hardness and increases the strength of martensitic weld joints. A strong negative correlation (Pearson correlation coefficient = -0.835) between hardness and strength was also obtained from the analysis of the data in Table 21.

Table 21. Properties of martensitic stainless steel at different post-weld treatment times [136].

Post-weld Treatment Time (Hour)	0	0.5	1	2
Ultimate Tensile Strength (MPa)	14.33	16.25	20.00	22.50
Hardness (HV)	375	252	239	225

Models were also developed for the mechanical properties of martensitic stainless steel in terms of ferrite composition, using the data in Table 19 by regression analysis. The summary of the model is given in Table 22 and the normal probability plots are given in Figure 3a–c.

2.4. Ferritic Stainless Steel

Ferritic stainless steel finds application in the automotive industry, fuel cells, catalytic converters, and the oil and gas industries, among others. The wide range of applications of ferritic stainless steel is attributed to their low cost, as compared to their counterpart austenitic stainless steel, strength, corrosion resistance, high temperature oxidation resistance, high thermal conductivity, low thermal expansion and weldability [140–143].

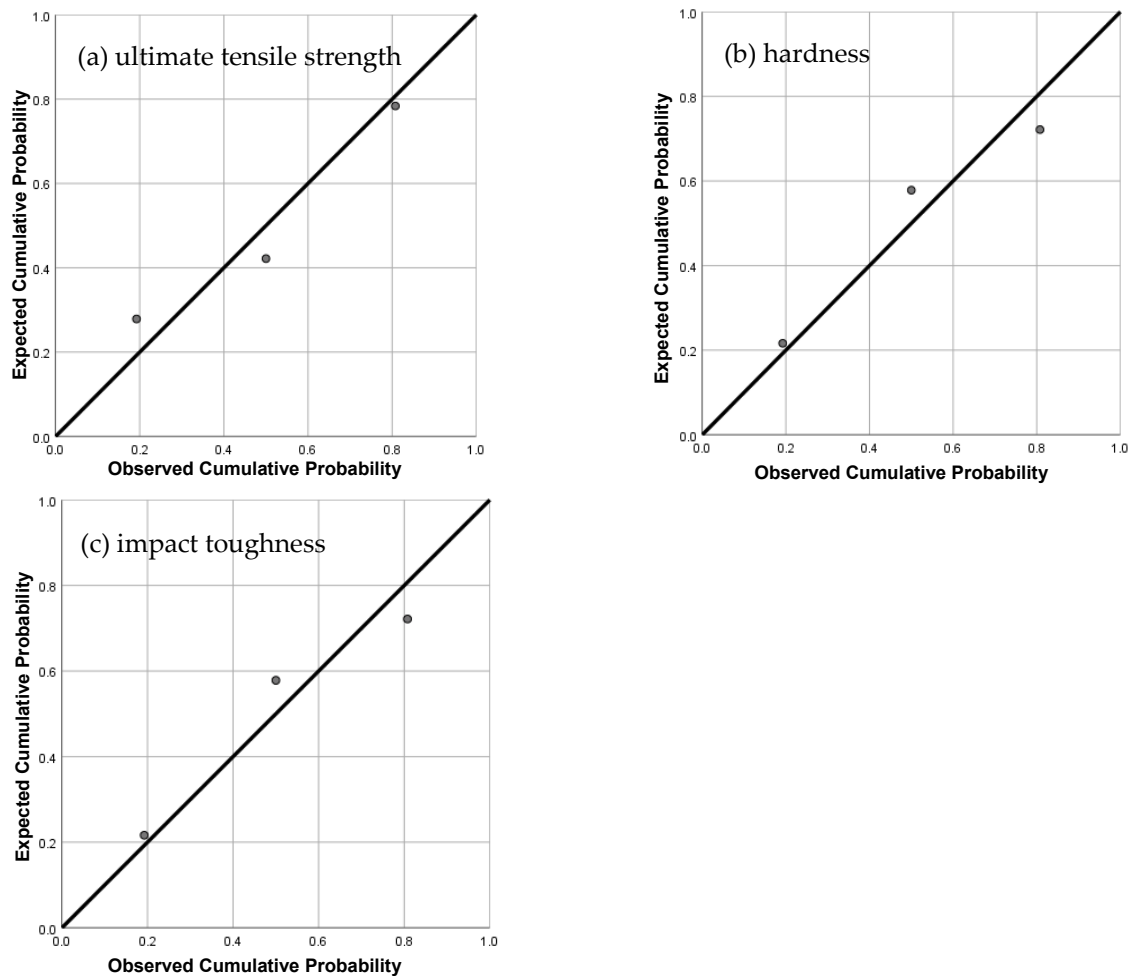
Welding ferritic stainless steel suffers some challenges, which includes the property deterioration of the weld metal, such as a reduction in fracture toughness, and the overall reduction in strength as a result of the thermal stress field which creates residual stresses in the weld metal [144]. The weld property obtained after welding is dependent on a number of factors, with the primary being the microstructure and chemical composition of the metal. The microstructure of ferritic stainless steel comprises ferrite and pearlite [145]. Table 23 shows the chemical composition of ferritic stainless steel. The application of appropriate microstructural modification processes such as post-weld heat treatment and plasma processing have been reported by researchers to improve the properties of welded ferritic stainless steel joints [146–148].

Table 22. Model summary for the mechanical properties of martensitic stainless steel in terms of ferrite composition.

Property	Model	R ²	Adjusted R ²
Ultimate Tensile Strength	$622.018 - 2.750F$	0.525	0.05
Hardness	$193.826 + 2.079F$	0.979	0.957
Impact Toughness	$16.850 + 3.313F$	0.769	0.538

Note that F in table denotes the percentage ferrite content.

redmine

**Figure 3.** Normal probability plots of the properties of martensitic stainless steel: (a) ultimate tensile strength; (b) hardness; (c) impact toughness.**Table 23.** Chemical composition of AISI 4140 ferritic stainless steel (% by weight) [145].

C	Cr	Mo	Mn	P	S	Si	Fe
0.38–0.43	0.8–1.1	0.15–0.25	0.75–1.0	0.035	0.04	0.15–0.3	balance

Grade 91 ferritic stainless steel, also known as chromium molybdenum ferritic stainless steel, is specifically used for high temperature applications, such as in boilers and heat exchangers in petrochemical and power plants, owing to its high temperature creep resistance and stress corrosion cracking, especially in corrosive environments [144]. Ahmed et al. [149] investigated the effect of annealing holding time on the properties of chromium molybdenum boiler ferritic stainless steel.

The results revealed that the ultimate tensile strength, yield strength, elongation and reduction in the area increases with holding time. The reduction observed in strength and ductility after a long holding time was as a result of spheroidization of pearlite grains. They also reported that the increase in impact energy with temperature and holding time was as a result of grain refinements coupled with the formation dendrites.

The effect of single and multiple tempering time on the properties of modified chromium molybdenum ferritic stainless steel was reported by Dey et al. [150] They found out that the yield strength and ultimate tensile strength decreases with single tempering holding time, as a result of martensite tempering coupled with the precipitation of fine precipitates, while multiple tempering time did not show any significant effect. This was accompanied by a corresponding increase in toughness and ductility. They also reported that the impact toughness increases with both single and multiple tempering time, and concluded that the tempering of welded ferritic stainless steel for a sufficient time can restore the properties, and that there was no need for multiple tempering time, as it had no significant improvement on the properties of the weld metal.

Taniguchi and Yamashita [151] studied the effect of manganese and nickel alloying additions on the properties of annealed grade 91 ferritic stainless steel. A reversal in mechanical properties—primarily tensile strength, absorbed energy and rupture time with annealing temperature, was observed in the samples with high content of manganese and nickel. This was attributed to the precipitation of fresh martensite at temperatures above the critical transformation temperature. A different trend was observed in samples with low alloy additions, as the tensile strength increased with temperature, while the absorbed energy decreased with temperature. The reason being that a small amount of fresh martensite is precipitated due to the presence of low alloying additions. They concluded that the upper limit post-weld heat treatment temperature for chromium molybdenum ferritic stainless steel is a function of the mechanical properties, and not the critical transformation temperature.

The application of post-weld heat treatments can sometimes be cost effective and time consuming. This led to the introduction of other property modification mechanisms such as electrolytic plasma processing (EPP). Property modification by EPP is as a result of the chemical, mechanical, electrical and thermal effect of the plasma produced at the surface [152,153]. Dewan et al. [145] investigated the effect of annealing, hardening and EPP on the properties of ferritic stainless steel.

Their findings revealed that, while annealing and hardening reduced and increased the hardness of the weld metal, respectively, EPP had no significant effect, as it is a surface mechanism and does not involve grain refinement. It has also been reported that EPP treatment reduces residual stresses induced during welding, but increases the compressive stresses, due to the thermal shock during the EPP process [154]. Maximum tensile strength was observed in the EPP treated samples, while hardening had no effect on tensile strength and ductility. The high tensile strength derived from the EPP treatment was due to the formation of surface martensite. From their findings, it was also discovered that the application of EPP treatment after annealing had no significant benefit in terms of property improvement, as it leads to increased compressive stresses and a reduction in toughness.

Conclusively, while increasing annealing temperature reduces the hardness of ferritic stainless steel, adequate annealing holding time increases ultimate tensile strength and the impact energy. Tempering, on the other hand, reduces the ultimate tensile strength due to martensite tempering, but increases toughness and ductility. Multiple tempering time did not show any significant difference in properties; therefore, it is not recommended. EPP, which is a surface modification mechanism, reduces residual stresses and increases tensile strength, due to fresh martensite precipitation. For high Cr heat resistant ferritic stainless steel, the upper critical limit for post-weld treatment is a function of the mechanical properties, and not the upper critical temperature.

Table 24 shows the properties of ferritic stainless steel at different annealing temperatures. A bivariate correlation analysis between properties and post-weld treatment temperature revealed that a perfect negative correlation exists between the annealing temperature and residual stresses. This implies that increasing annealing temperature would eliminate the residual stresses induced by

welding. A moderate correlation between hardness and strength was observed, as can be seen in Table 25.

Table 24. Properties of ferritic stainless steel at different annealing temperatures [145].

Temperature (°C)	24	500	650
Residual Stress (MPa)	450	280	160
Hardness (HB)	425	365	340
Ultimate Tensile Strength (MPa)	839.2	837.7	774.5

Table 25. Pearson correlation coefficient between properties of ferritic stainless steel and annealing temperature.

	Residual Stress (MPa)	Ultimate Tensile Strength (MPa)
Temperature(°C)	-0.981	
Hardness (HB)		0.661

Table 26 shows the summary of the mathematical model of residual stress developed at the fusion zone of ferritic stainless steel in terms of annealing temperature, and Figure 4 shows the normal probability plot.

Table 26. Model for residual stress of ferritic stainless steel in terms of annealing temperature (T).

Property	Model	R ²	Adjusted R ²
Residual Stress (MPa)	$467.902 - 0.438T$	0.963	0.927

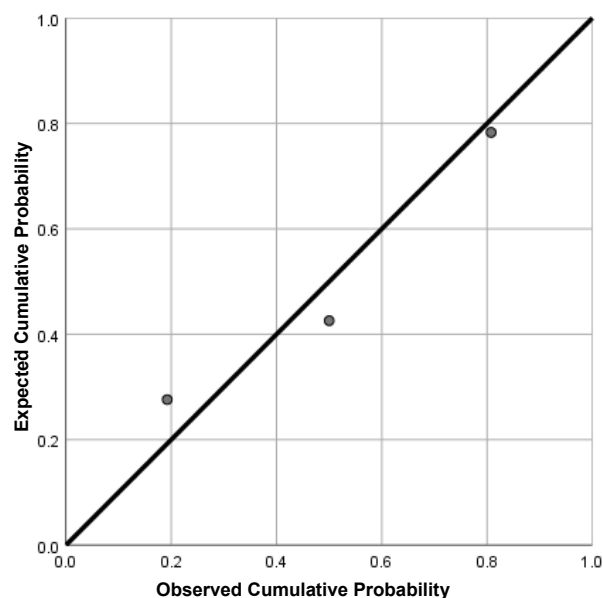


Figure 4. Normal probability plot for residual stress of ferritic stainless steel.

3. Dissimilar Welding of Stainless Steel with Other Metals

Dissimilar welding involves creating dissimilar joints of stainless steel and other metals. A review of the literature of the dissimilar welding of stainless steel revealed that most of the dissimilar joints involve austenitic stainless steel. This form of welding is carried out in order to optimize the properties conferred by each base metal, with the objective of minimizing cost and obtaining excellent service performance [155]. Dissimilar welding is used in petroleum industries, chemical plants, ITER

components, nuclear plants and aerospace industries [156–158]. The major challenge faced during the dissimilar welding of stainless steel is the difference in thermophysical and chemical composition of the base metals, which results in intermetallic phase precipitation, residual stress generation and overall property deterioration; hence, the need for pre- and post-weld treatment [159–164].

3.1. Austenitic Stainless Steel, Carbon Steel and Cast Iron

Carbon steel possesses good strength and wear resistance, and it is quite cheap, while cast iron, on the other hand, has a good combination of strength and toughness. The dissimilar joints of these metals with stainless steel are desired because of its strength and corrosion resistance. Austenitic stainless steel-carbon steel joints find applications in boilers, oil and gas industries and thermal power plants, while the latter is used in the automobile industry and general machinery [165,166].

The microstructure of carbon steel comprises pearlite dispersed in a ferrite matrix, while that of ductile cast iron consist of graphite embedded in a ferritic and pearlitic matrix [2,167]. Tables 27 and 28 contain the chemical composition of carbon steel and ductile cast iron, respectively.

Table 27. Chemical composition of 1045 carbon steel (% by weight) [2].

C	Si	Mn	Ni	Cr	Fe
0.42–0.5	0.17–0.37	0.5–0.8	<0.25	<0.25	balance

Table 28. Chemical composition of FCD450 ductile cast iron (% by mass) [166].

C	Mg	Mn	P	S	Si	Fe
3.32	0.043	0.23	0.029	0.006	2.77	balance

The property obtained from the dissimilar weld joint is a function of the chemical composition and microstructure of the base metals, among other factors. The major difficulty encountered in the welding of stainless steel-carbon steel is the formation of chromium carbide, which is accompanied by the decarburization of the carbon steel, leading to the deterioration in mechanical properties and the reduction in corrosion resistance [30,168]. Stainless steel–cast iron joints, on the other hand, face the challenge of poor weldability coupled with the precipitation of ledeburite, which increases hardness of the weld joints and eventually leads to failure [167,169]. The application of adequate weld treatment processes can improve the property of welded joints.

The effect of annealing temperature on the properties of the dissimilar joint of 1045 carbon steel and 304 austenitic stainless steel was investigated by Ma et al. [2] The result of their experiment revealed that increasing annealing temperature increases carbide precipitation, due to an increase in the diffusion rate of carbon atoms. This was also accompanied by an increase in the hardness of the fusion zone and a corresponding decrease in corrosion resistance, owing to the depletion in chromium content. However, at low annealing temperatures, the reduction in fusion zone hardness was reported as a result of the increase in ferrite content, reduced dislocation density and coarse austenite grains. Though the tensile strength fluctuated with increasing annealing temperatures, the maximum strength of the joint obtained was approximately equivalent to that of the stainless steel base metal. They also reported no significant changes in the microstructure of the stainless steel base metal, as the post-weld treatment temperatures were below the transformation temperature.

Similar results were also reported by Sadeghi et al. [165], who studied the effect of annealing temperature on the properties of the A537CL1 carbon steel pressure vessel and A321 austenitic stainless steel dissimilar joint. They reported that the ultimate tensile strength, yield strength, ductility, toughness and impact energy decreased with increasing annealing temperatures. This reduction in mechanical properties at high annealing temperatures was due to the carbide precipitation. The residual stresses, though, reduced at low annealing temperatures, but with increasing annealing temperatures, it was found to increase. This resulted from the difference in thermal expansion of the base metals.

It can be deduced from their findings that optimum mechanical properties are obtained at low annealing temperatures.

Sawada and Nakamura investigated the effect of preheating temperature, tool speed and welding speed on the properties of austenitic stainless steel and ductile cast iron dissimilar joint [166]. The results of their findings revealed that the hardness of the fusion zone increased with increasing preheating temperature, due to martensite precipitation and chilling. Chilling is a term used to refer to the appearance of cementite in cast iron, and it has been reported to cause embrittlement [170,171]. The tensile strength was also reported to increase with increasing preheating temperature and welding speed. This was the result of an increase in deformed layer of spheroidal graphite (DLSG), chill reduction and reduction in martensite precipitation.

3.2. Austenitic, Ferritic and Martensitic Stainless Steel

Ferritic stainless steel is flexible, cheap, and possesses good corrosion resistance. Their dissimilar joints with austenitic stainless steel have applications in the power industry, petrochemical industry and oil and gas industry. Martensitic stainless steel, on the other hand, possesses void swelling resistance and good thermophysical and thermomechanical properties. Their dissimilar joints with austenitic stainless steel are major structural elements used in the test blanket system (TBS) [172–175]. The dissimilar welding of austenitic stainless steel to martensitic stainless steel suffers the challenge of martensite transformation on the martensitic stainless steel side, which results in hardening, and hence, the need for post-weld treatment. Austenitic-ferritic stainless steel joints, on the other hand, face the challenge of carbide precipitation, which leads to weld property deterioration including corrosion resistance.

Researchers have reported several methods of reducing carbide precipitation in these joints, some of which include the use of a low energy input welding technique, the addition of alloying elements with a high affinity for carbon, such as vanadium, titanium and niobium, and the use of adequate post-weld heat treatment. It has also been reported that the use of adequate post-weld treatment is less cost intensive when compared to its counterparts [176–178].

Ghorbani et al. [179] investigated the effect of annealing temperature and filler electrode on the properties of AISI304L austenitic stainless steel and AISI430 ferritic stainless steel dissimilar joints. The results of their findings revealed that the tensile strength and ductility increases with annealing temperature, as a result of carbide precipitation at elevated temperatures and a reduction in the delta ferrite composition of the weld metal. The corrosion resistance was found to diminish with annealing temperature and the use of the ferritic or austenitic filler electrode.

A reduction in corrosion resistance was attributed to the martensite formation due to the fast cooling rate, while the formation of secondary phases such as sigma phase and sulphides with the use of ferritic and austenitic filler electrodes led to a reduction in corrosion resistance.

The effect of tempering temperature on the properties of CLAM/316L dissimilar joints was studied by Zhang et al. [180] They reported that the hardness of the dissimilar joints reduced with tempering temperature due to martensite tempering, while the tensile strength fluctuated with tempering temperature as a result of the precipitation, dissolution and re-precipitation of carbides. They also reported a low impact energy for the dissimilar joints; lower than both base metals.

3.3. Austenitic Stainless Steel, Titanium and Nickel Alloy

Titanium and nickel alloys belong to the family of shape memory alloys and find application in aerospace industry and biomedical instruments, due to their ability to recover their original shape after mechanical deformation (pseudo-elasticity), and their ability to retain the deformed shape up to their recovery temperature (shape memory effect) [181–185]. The limited use of titanium and its alloys is due to its expensive nature, and consequently, it is welded with stainless steel to reduce the cost and extend its range of applications [33].

The microstructure of titanium-nickel alloys contains about 45% titanium and 55% nickel, while pure titanium metal contains about 99% titanium with other alloying additions [186,187]. The major challenge encountered in their dissimilar welding with stainless steel, aside the general difficulty encountered in producing good quality joints, is the precipitation of deleterious intermetallic phases [188]. Secondary phase precipitation can be minimized by incorporating an interlayer, which can be an aluminum, copper, silver or nickel-based filler metal [188,189]. General property modification of the weld joints is achieved by applying appropriate post-weld treatment.

Chen et al. [190] investigated the effect of high annealing temperature (650–850 °C) on the properties of NiTi/304SS dissimilar joints. The results of their findings revealed that the tensile strength, elongation and microhardness increases with annealing temperature. The improvement in mechanical properties was attributed to the precipitation of intermetallic phases. The effect of low annealing temperature (200–400 °C) was investigated by Mirshekari et al. [191] They reported an improved tensile strength and hardness due to the release of residual stresses and less precipitation of intermetallic phases. They also reported that better corrosion resistance is exhibited at low annealing temperatures, due to the disruption of the sessile dislocation networks, which are pitting corrosion sites in addition to less precipitation of intermetallics and residual stress release [192,193].

The effect of preheating, friction welding parameters and surface condition on the properties of cp-titanium/316L dissimilar weld was studied by Akbarimousavi and Goharikia [194]. The results of their experiments revealed that samples with surface smoothening followed by cleaning with acetone had the best tensile properties. This is an indication that these joints are very sensitive to the surface conditions of the base metals prior to welding. Surface cleaning eliminates intermetallics, which have been reported to cause reduction in strength of welded joints due to their brittle nature [195,196]. They also discovered that increasing forging pressure eliminates intermetallics from the weld interface to the flash region.

3.4. Austenitic Stainless Steel, Copper and Aluminium Alloy

Copper has a high thermal and electrical conductivity and resistance to corrosion, and it is malleable. These properties are combined with the strength and corrosion resistance of stainless steel in a dissimilar weld joint, which finds application in nuclear power plants [197,198]. Aluminum, on the other hand, is light, and its dissimilar joint with stainless steel is desired when weight reduction is the design priority, like in the automobile and aerospace industries.

The microstructure of copper and aluminum contains about 98% of the pure metal, with about 2% alloying additions [199,200]. Creating dissimilar joints of copper/stainless steel and aluminium/stainless steel has posed a great challenge for some decades now. Though some researchers have reported to have fabricated joints with good strength using some low heat input welding techniques, the properties obtained from such joints does not meet the minimum mechanical requirements, hence, they have limited applications [201–207]. In order to obtain joints with improved mechanical properties, a combination of two or more welding techniques, known as hybrid welding, has been attempted by several researchers with several post-weld treatment processes [208,209].

The hybrid welding of copper/stainless steel dissimilar joints with gas tungsten arc welding assisted heating and external cooling was investigated by Joshi and Badheka [210]. They observed that deformation (in the form of flash) and oxidation (in form of black stirred surface) increased with preheating temperature. A similar result was reported by Mofid et al. [211] The low oxidation rate observed at low temperatures is due to the formation of a water blanket on the surface of the stirred metal, as reported by Zhang et al. [212] The tensile strength was also observed to deteriorate with assisted heating or cooling, due to the high rate of deformation at elevated temperatures, and the low copper/stainless steel bond strength at low temperatures. They concluded that, though assisted heating and cooling reduced the hardness of the stir zone, optimum weld properties for copper/stainless steel joints are obtained in the as weld condition, without assisted heating or cooling.

The effect of hybrid welding and tool rotation speed on the properties of aluminum alloy/stainless steel dissimilar joints was studied by Bang et al. [213] From their findings, it was discovered that joints with good strength almost equal to that of the aluminum base metal was obtained at an intermediate tool rotation speed using hybrid welding. They also found out that the maximum reduction in hardness of the stir zone was obtained with hybrid welding, which was attributed to the refinement of grain size by preheating coupled with the reduction in dislocation density.

Dong et al. [214] studied the effect of post-weld heat treatment and holding time on the properties of aluminum alloy/stainless steel dissimilar joint welded, using the zinc based filler electrode. The result of their findings revealed that the interfacial layer thickness increases with post-weld treatment temperature, due to the increase in precipitation of zinc rich phases coupled with the increase in diffusion rate of aluminum and iron to the interfacial layer. They also reported a fluctuation in the tensile strength with temperature and holding time, due to a fluctuation in the precipitation of fine zinc rich phases at the interfacial layer, and concluded that optimum joint properties are obtained at intermediate holding times and post-weld temperatures.

4. Conclusions

As a sequel to the review of the effect of pre- and post-weld treatments on the properties of stainless steel, and subsequently, their microstructure-property correlation, the following conclusions were made.

1. The properties of austenitic stainless steel are very sensitive to the presence of the delta ferrite phase. Preheating temperature, annealing temperature and holding time were found to be negatively correlated with the delta ferrite composition, which is an indication of delta ferrite phase transformation to sigma phase at high temperatures. Meanwhile, the tensile strength, hardness and corrosion current density showed a positive correlation. A moderate positive correlation was also exhibited between hardness and tensile strength.
2. Optimum properties in duplex stainless steel weld joints are obtained when the ferrite-austenite ratio was close to unity. This ratio was found to be positively correlated with hardness and negatively correlated with ultimate tensile strength and corrosion current density. The ferrite phase stabilizers were also found to be positively correlated with the ultimate tensile strength.
3. Martensitic stainless steel weld joint properties are a function of the microstructure which contains martensite, ferrite and austenite phases. The ferrite phase was found to be positively correlated with the hardness and impact toughness and negatively correlated with the tensile strength. A negative correlation was also observed between the hardness and ultimate tensile strength.
4. General property deterioration at the weld joint due to induced stresses is a major setback encountered during the fabrication of ferritic stainless steel. Residual stress was found to be perfectly negatively correlated with temperature, while the ultimate tensile strength was positively correlated with the hardness of the weld joint. This suggests that residual stresses induced by the welding process are eliminated at high temperatures of post-weld treatment.
5. The major difficulty encountered in producing stainless steel dissimilar joints is the difference in thermophysical properties and chemical composition of the base metals, which results in intermetallic phase precipitation, and ultimately, property deterioration, primarily at the weld joint. Improved properties can be obtained by the use of an appropriate welding technique, the application of an adequate weld treatment process, the use of alloy additions, and the incorporation of an interlayer.

Author Contributions: M.M. (Musa Muhammed) made the major contribution to the paper and also wrote the paper, M.M. (Mazli Mustapha) and T.L.G. designed the methodology for data analysis and the structure of the paper, A.M.A. performed the statistical analysis while F.M. and C.C.H. discussed the results of the analysis. All authors have read and agreed to the published version of the manuscript.

Funding: This research was funded by the Yayasan Universiti Teknologi Petronas under the YUTP-Fundamental Research Grant Scheme (Cost center: 05LCO-052).

Acknowledgments: The authors want to thank Universiti Teknologi PETRONAS for their necessary support throughout the project. We also want to acknowledge the support of the Yayasan Universiti Teknologi Petronas under the YUTP-Fundamental Research Grant Scheme (Cost center: 015LCO-052).

Conflicts of Interest: The authors declare no conflict of interest.

References

- Zareie Rajani, H.R.; Torkamani, H.; Sharbati, M.; Raygan, S. Corrosion resistance improvement in Gas Tungsten Arc Welded 316L stainless steel joints through controlled preheat treatment. *Mater. Des.* **2012**, *34*, 51–57. [[CrossRef](#)]
- Ma, H.; Qin, G.; Geng, P.; Li, F.; Meng, X.; Fu, B. Effect of post-weld heat treatment on friction welded joint of carbon steel to stainless steel. *J. Mater. Process. Technol.* **2016**, *227*, 24–33. [[CrossRef](#)]
- Al-Mukhtar, A.M.; Al-Jumaili, S.A.K.; Al-Jleahwy, A.H.F. Effect of Heat Treatments on 302 Austenitic Stainless Steel Spot Weld. *Adv. Eng. Forum.* **2018**, *29*, 19–25. [[CrossRef](#)]
- Movahed, P.; Kolahgar, S.; Marashi, S.P.H.; Pouranvari, M.; Parvin, N. The effect of intercritical heat treatment temperature on the tensile properties and work hardening behavior of ferrite-martensite dual phase steel sheets. *Mater. Sci. Eng. A* **2009**, *518*, 1–6. [[CrossRef](#)]
- Lin, Y.C.; Chen, S.C. Effect of residual stress on thermal fatigue in a type 420 martensitic stainless steel weldment. *J. Mater. Process. Technol.* **2003**, *138*, 22–27. [[CrossRef](#)]
- Baldev, R.; Choudhary, B.K.; Raman, R.K.S. Mechanical properties and non-destructive evaluation of Cr-Mo ferritic steels for steam generator application. *Int. J. Press. Vessel. Pip.* **2004**, *81*, 521–534. [[CrossRef](#)]
- Foussat, A.; Weiyue, W.; Jing, W.; Shuang song, D.; Sgobba, S.; Hongwei, L.; Libeyre, P.; Jong, C.; Klofac, K.; Mitchell, N. Mechanical design and construction qualification program on ITER correction coils structures. *Nucl. Eng. Des.* **2014**, *269*, 116–124. [[CrossRef](#)]
- Marshall, A.W.; Farrar, J.C.M. Welding of ferritic and martensitic 11–14% Cr steels. *Weld. World.* **2001**, *45*, 32–55.
- Tan, H.; Jiang, Y.; Deng, B.; Sun, T.; Xu, J.; Li, J. Effect of annealing temperature on the pitting corrosion resistance of super duplex stainless steel UNS S32750. *Mater. Charact.* **2009**, *60*, 1049–1054. [[CrossRef](#)]
- Chandravathi, K.S.; Laha, K.; Bhanu Sankara Rao, K.; Mannan, S.L. Microstructure and tensile properties of modified 9Cr-1Mo steel (grade 91). *Mater. Sci. Technol.* **2001**, *17*, 559–565. [[CrossRef](#)]
- Kozuh, S.; Gojic, M.; Kosec, L. Mechanical properties and microstructure of austenitic stainless steel after welding and post-weld heat treatment. *Kov. Mater.* **2009**, *47*, 253–262.
- Nayak, S.S.; Zhou, Y.; Baltazar Hernandez, V.H.; Biro, E. Resistance spot welding of dual-phase steels: Heat affected zone softening and tensile properties. In Proceedings of the 9th International Conference on Trends in Welding Research, Chicago, IL, USA, 4–8 June 2012; pp. 641–649.
- Bhamji, I.; Preuss, M.; Threadgill, P.L.; Moat, R.J.; Addison, A.C.; Peel, M.J. Linear friction welding of AISI 316L stainless steel. *Mater. Sci. Eng. A* **2010**, *528*, 680–690. [[CrossRef](#)]
- Muhammad, F.; Ahmad, A.; Farooq, A.; Haider, W. Effect of Post-Weld Heat Treatment on Mechanical and Electrochemical Properties of Gas Metal Arc-Welded 316L (X2CrNiMo 17-13-2) Stainless Steel. *J. Mater. Eng. Perform.* **2016**, *25*, 4283–4291. [[CrossRef](#)]
- Zhang, C.; Zhao, S.; Sun, X.; Sun, D.; Sun, X. Corrosion of laser-welded NiTi shape memory alloy and stainless steel composite wires with a copper interlayer upon exposure to fluoride and mechanical stress. *Corros. Sci.* **2014**, *82*, 404–409. [[CrossRef](#)]
- Tabatabaeipour, S.M.; Honarvar, F. A comparative evaluation of ultrasonic testing of AISI 316L welds made by shielded metal arc welding and gas tungsten arc welding processes. *J. Mater. Process. Technol.* **2010**, *210*, 1043–1050. [[CrossRef](#)]
- Kar, J.; Roy, S.K.; Roy, G.G. Effect of beam oscillation on electron beam welding of copper with AISI-304 stainless steel. *J. Mater. Process. Technol.* **2016**, *233*, 174–185. [[CrossRef](#)]
- Huang, H.Y. Research on the activating flux gas tungsten Arc welding and plasma Arc welding for stainless steel. *Met. Mater. Int.* **2010**, *16*, 819–825. [[CrossRef](#)]

19. Vural, M.; Akkuş, A.; Eryürek, B. Effect of welding nugget diameter on the fatigue strength of the resistance spot welded joints of different steel sheets. *J. Mater. Process. Technol.* **2006**, *176*, 127–132. [[CrossRef](#)]
20. Ananthapadmanaban, D.; Seshagiri Rao, V.; Abraham, N.; Prasad Rao, K. A study of mechanical properties of friction welded mild steel to stainless steel joints. *Mater. Des.* **2009**, *30*, 2642–2646. [[CrossRef](#)]
21. Zhou, X.; Chen, Y.; Huang, Y.; Mao, Y.; Yu, Y. Effects of niobium addition on the microstructure and mechanical properties of laser-welded joints of NiTiNb and Ti6Al4V alloys. *J. Alloys Compd.* **2018**, *735*, 2616–2624. [[CrossRef](#)]
22. Modenesi, P.J.; Apolinário, E.R.; Pereira, I.M. TIG welding with single-component fluxes. *J. Mater. Process. Technol.* **2000**, *99*, 260–265. [[CrossRef](#)]
23. Li, J.; Guan, Q.; Shi, Y.W.; Guo, D.L. Stress and distortion mitigation technique for welding titanium alloy thin sheet. *Sci. Technol. Weld. Join.* **2004**, *9*, 451–458. [[CrossRef](#)]
24. Ureña, A.; Otero, E.; Utrilla, M.V.; Múñez, C.J. Weldability of a 2205 duplex stainless steel using plasma arc welding. *J. Mater. Process. Technol.* **2007**, *182*, 624–631. [[CrossRef](#)]
25. Luo, J.; Yuan, Y.; Wang, X.; Yao, Z. Double-sided single-pass submerged arc welding for 2205 duplex stainless steel. *J. Mater. Eng. Perform.* **2013**, *22*, 2477–2486. [[CrossRef](#)]
26. Gunaraj, V.; Murugan, N. Prediction and comparison of the area of the heat-affected zone for the bead-on-plate and bead-on-joint in submerged arc welding of pipes. *J. Mater. Process. Technol.* **1999**, *95*, 246–261. [[CrossRef](#)]
27. Srivastava, B.K.; Tewari, D.S.P.; Jyoti, P. A Review on the Effects of preheating and/or post weld treatment on the mechanical behaviour of Ferrous metals. *Int. J. Eng. Sci. Technol.* **2010**, *2*, 625–631.
28. Tseng, C.C.; Shen, Y.; Thompson, S.W.; Mataya, M.C.; Krauss, G. Fracture and the formation of sigma phase, M23C6, and austenite from delta-ferrite in an AISI 304L stainless steel. *Metall. Mater. Trans. A.* **1994**, *25*, 1147–1158. [[CrossRef](#)]
29. Pouranvari, M.; Marashi, S.P.H. Critical review of automotive steels spot welding: Process, structure and properties. *Sci. Technol. Weld. Join.* **2013**, *18*, 361–403. [[CrossRef](#)]
30. Marashi, P.; Pouranvari, M.; Amirabdollahian, S.; Abedi, A.; Goodarzi, M. Microstructure and failure behavior of dissimilar resistance spot welds between low carbon galvanized and austenitic stainless steels. *Mater. Sci. Eng. A* **2008**, *480*, 175–180. [[CrossRef](#)]
31. Zhang, B.G.; Zhao, J.; Li, X.P.; Chen, G.Q. Effects of filler wire on residual stress in electron beam welded QCr0.8 copper alloy to 304 stainless steel joints. *Appl. Therm. Eng.* **2015**, *80*, 261–268. [[CrossRef](#)]
32. Akbari Mousavi, S.A.A.; Sartangi, P.F. Effect of post-weld heat treatment on the interface microstructure of explosively welded titanium-stainless steel composite. *Mater. Sci. Eng. A* **2008**, *494*, 329–336. [[CrossRef](#)]
33. Li, Q.; Zhu, Y. Impact butt welding of NiTi and stainless steel- An examination of impact speed effect. *J. Mater. Process. Technol.* **2018**, *255*, 434–442. [[CrossRef](#)]
34. Çetin, A.; Tek, Z.; Öztarhan, A.; Artunç, N. A comparative study of single and duplex treatment of martensitic AISI 420 stainless steel using plasma nitriding and plasma nitriding-plus-nitrogen ion implantation techniques. *Surf. Coatings Technol.* **2007**, *201*, 8127–8130. [[CrossRef](#)]
35. Garcia, C.; de Tiedra, M.P.; Blanco, Y.; Martin, O.; Martin, F. Intergranular corrosion of welded joints of austenitic stainless steels studied by using an electrochemical minicell. *Corros. Sci.* **2008**, *50*, 2390–2397. [[CrossRef](#)]
36. Khan, M.M.A.; Romoli, L.; Dini, G. Laser beam welding of dissimilar ferritic/martensitic stainless steels in a butt joint configuration. *Opt. Laser Technol.* **2013**, *49*, 125–136. [[CrossRef](#)]
37. Sathiya, P.; Mishra, M.K.; Shanmugarajan, B. Effect of shielding gases on microstructure and mechanical properties of super austenitic stainless steel by hybrid welding. *Mater. Des.* **2012**, *33*, 203–212. [[CrossRef](#)]
38. Chen, Y.B.; Lei, Z.L.; Li, L.Q.; Wu, L. Experimental study on welding characteristics of CO2 laser TIG hybrid welding process. *Sci. Technol. Weld. Join.* **2006**, *11*, 403–411. [[CrossRef](#)]
39. Yan, J.; Gao, M.; Zeng, X. Study on microstructure and mechanical properties of 304 stainless steel joints by TIG, laser and laser-TIG hybrid welding. *Opt. Lasers Eng.* **2010**, *48*, 512–517. [[CrossRef](#)]
40. Çetinarıslan, C.S.; Sahin, M.; Genc, S.K.; Sevil, C. Mechanical and metallurgical properties of ion-nitrided austenitic-stainless steel welds. *Mater. Sci. Pol.* **2012**, *30*, 303–312. [[CrossRef](#)]
41. Alphonsa, J.; Padsala, B.A.; Chauhan, B.J.; Jhala, G.; Rayjada, P.A.; Chauhan, N.; Soman, S.N.; Raole, P.M. Plasma nitriding on welded joints of AISI 304 stainless steel. *Surf. Coatings Technol.* **2013**, *228*, S306–S311. [[CrossRef](#)]

42. Sun, Y.F.; Shen, J.M.; Morisada, Y.; Fujii, H. Spot friction stir welding of low carbon steel plates preheated by high frequency induction. *Mater. Des.* **2014**, *54*, 450–457. [[CrossRef](#)]
43. Sánchez-Cabrera, V.M.; Rubio-González, C.; Ruíz-Vela, J.I.; Ramírez-Baltazar, C. Effect of preheating temperature and filler metal type on the microstructure, fracture toughness and fatigue crack growth of stainless steel welded joints. *Mater. Sci. Eng. A* **2007**, *452–453*, 235–243. [[CrossRef](#)]
44. Chen, Y.; Song, X.; Zhou, J.; Liu, H.; Yang, Y. The study on the overall plasma electrolytic oxidation for 6061-7075 dissimilar aluminum alloy welded parts based on the dielectric breakdown theory. *Materials (Basel)* **2018**, *11*, 63. [[CrossRef](#)] [[PubMed](#)]
45. Tan, H.; Wang, Z.; Jiang, Y.; Han, D.; Hong, J.; Chen, L.; Jiang, L.; Li, J. Annealing temperature effect on the pitting corrosion resistance of plasma arc welded joints of duplex stainless steel UNS S32304 in 1.0M NaCl. *Corros. Sci.* **2011**, *53*, 2191–2200. [[CrossRef](#)]
46. Parvathavarthini, N.; Dayal, R.K.; Khatak, H.S.; Shankar, V.; Shanmugam, V. Sensitization behaviour of modified 316N and 316L stainless steel weld metals after complex annealing and stress relieving cycles. *J. Nucl. Mater.* **2006**, *355*, 68–82. [[CrossRef](#)]
47. Badji, R.; Bouabdallah, M.; Bacroix, B.; Kahloun, C.; Belkessa, B.; Maza, H. Phase transformation and mechanical behavior in annealed 2205 duplex stainless steel welds. *Mater. Charact.* **2008**, *59*, 447–453. [[CrossRef](#)]
48. Tseng, K.H. Development and application of oxide-based flux powder for tungsten inert gas welding of austenitic stainless steels. *Powder Technol.* **2013**, *233*, 72–79. [[CrossRef](#)]
49. Sathiya, P.; Aravindan, S.; Noorul Haq, A. Effect of friction welding parameters on mechanical and metallurgical properties of ferritic stainless steel. *Int. J. Adv. Manuf. Technol.* **2007**, *31*, 1076–1082. [[CrossRef](#)]
50. Thibault, D.; Bocher, P.; Thomas, M. Residual stress and microstructure in welds of 13%Cr-4%Ni martensitic stainless steel. *J. Mater. Process. Technol.* **2009**, *209*, 2195–2202. [[CrossRef](#)]
51. Saeid, T.; Abdollah-zadeh, A.; Shibayanagi, T.; Ikeuchi, K.; Assadi, H. On the formation of grain structure during friction stir welding of duplex stainless steel. *Mater. Sci. Eng. A* **2010**, *527*, 6484–6488. [[CrossRef](#)]
52. Goyal, S.; Sandhya, R.; Valsan, M.; Bhanu Sankara Rao, K. The effect of thermal ageing on low cycle fatigue behaviour of 316 stainless steel welds. *Int. J. Fatigue.* **2009**, *31*, 447–454. [[CrossRef](#)]
53. Chen, X.H.; Lu, J.; Lu, L.; Lu, K. Tensile properties of a nanocrystalline 316L austenitic stainless steel. *Scr. Mater.* **2005**, *52*, 1039–1044. [[CrossRef](#)]
54. Geantă, V.; Voiculescu, I.; Stefănoiu, R.; Rusu, E.R. Stainless steels with biocompatible properties for medical devices. *Key Eng. Mater.* **2014**, *583*, 9–15. [[CrossRef](#)]
55. Liverani, E.; Toschi, S.; Ceschini, L.; Fortunato, A. Effect of selective laser melting (SLM) process parameters on microstructure and mechanical properties of 316L austenitic stainless steel. *J. Mater. Process. Technol.* **2017**, *249*, 255–263. [[CrossRef](#)]
56. Conejero, O.; Palacios, M.; Rivera, S. Premature corrosion failure of a 316L stainless steel plate due to the presence of sigma phase. *Eng. Fail. Anal.* **2009**, *16*, 699–704. [[CrossRef](#)]
57. Nam, T.H.; An, E.; Kim, B.J.; Shin, S.; Ko, W.S.; Park, N.; Kang, N.; Jeon, J.B. Effect of post weld heat treatment on the microstructure and mechanical properties of a submerged-arc-welded 304 stainless steel. *Metals (Basel)* **2018**, *8*, 26. [[CrossRef](#)]
58. Lippold, J.; Kotecki, D. *Welding Metallurgy and Weldability of Stainless Steels*; Wiley-VCH: Weinheim, Germany, 2005; pp. 58–60.
59. Hamada, I.; Yamauchi, K. Sensitization behavior of type 308 stainless steel weld metals after postweld heat treatment and low-temperature aging and its relation to microstructure. *Metall. Mater. Trans. A Phys. Metall. Mater. Sci.* **2002**, *33*, 1743–1754. [[CrossRef](#)]
60. Sahlaoui, H.; Sidhom, H. Experimental investigation and analytical prediction of σ -phase precipitation in AISI 316L austenitic stainless steel. *Metall. Mater. Trans. A Phys. Metall. Mater. Sci.* **2013**, *44*, 3077–3083. [[CrossRef](#)]
61. Sahlaoui, H.; Sidhom, H.; Philibert, J. Prediction of chromium depleted-zone evolution during aging of Ni-Cr-Fe alloys. *Acta Mater.* **2002**, *50*, 1383–1392. [[CrossRef](#)]
62. Deo, M.V.; Michaleris, P.; Sun, J. Prediction of buckling distortion of welded structures. *Sci. Technol. Weld. Join.* **2003**, *8*, 55–61. [[CrossRef](#)]
63. Deo, M.V.; Michaleris, P. Mitigation of welding induced buckling distortion using transient thermal tensioning. *Sci. Technol. Weld. Join.* **2003**, *8*, 49–54. [[CrossRef](#)]

64. Venkata, K.A.; Kumar, S.; Dey, H.C.; Smith, D.J.; Bouchard, P.J.; Truman, C.E. Study on the effect of post weld heat treatment parameters on the relaxation of welding residual stresses in electron beam welded P91 steel plates. *Procedia Eng.* **2014**, *86*, 223–233. [[CrossRef](#)]
65. Yuan, X.; Chen, L.; Zhao, Y.; Di, H.; Zhu, F. Influence of annealing temperature on mechanical properties and microstructures of a high manganese austenitic steel. *J. Mater. Process. Technol.* **2015**, *217*, 278–285. [[CrossRef](#)]
66. Rosen, C.J.; Gumenyuk, A.; Zhao, H.; Dilthey, U. Influence of local heat treatment on residual stresses in electron beam welding. *Sci. Technol. Weld. Join.* **2007**, *12*, 614–619. [[CrossRef](#)]
67. Jia, W.T.; Zhao, J.P.; Cao, J. The Mitigation of Weld Residual Stress on 304L Stainless Steel by Post Weld Cool Treatment Process. *Appl. Mech. Mater.* **2016**, *853*, 209–215. [[CrossRef](#)]
68. Xin, J.; Fang, C.; Song, Y.; Wei, J.; Xu, S.; Wu, J. Effect of post weld heat treatment on the microstructure and mechanical properties of ITER-grade 316LN austenitic stainless steel weldments. *Cryogenics (Guildf)* **2017**, *83*, 1–7. [[CrossRef](#)]
69. Oluwatobi, E.M. Effect of Pre and Post-Heattreatment on the Heat-Affected-Zone (HAZ) of Austenitic Stainless-Steel. Bachelor's Thesis, Novia University of Applied Sciences, Vaasa, Finland, 2017.
70. Sathiya, P.; Aravindan, S.; Soundararajan, R.; Noorul Haq, A. Effect of shielding gases on mechanical and metallurgical properties of duplex stainless-steel welds. *J. Mater. Sci.* **2009**, *44*, 114–121. [[CrossRef](#)]
71. Theofanous, M.; Gardner, L. Experimental and numerical studies of lean duplex stainless steel beams. *J. Constr. Steel Res.* **2010**, *66*, 816–825. [[CrossRef](#)]
72. De Abreu, M.; Iordachescu, M.; Valiente, A. Effects of hydrogen assisted stress corrosion on damage tolerance of a high-strength duplex stainless steel wire for prestressing concrete. *Constr. Build. Mater.* **2014**, *66*, 38–44. [[CrossRef](#)]
73. Zhang, Z.; Zhang, H.; He, L.; Han, D.; Jiang, Y.; Li, J. Precipitation evolution in duplex stainless steel during isothermal aging at 700 °C. *Mater. Sci. Technol. (UK)* **2014**, *30*, 451–457. [[CrossRef](#)]
74. Medina, E.; Medina, J.M.; Cobo, A.; Bastidas, D.M. Evaluation of mechanical and structural behavior of austenitic and duplex stainless steel reinforcements. *Constr. Build. Mater.* **2015**, *78*, 1–7. [[CrossRef](#)]
75. Yang, L.; Zhao, M.; Chan, T.M.; Shang, F.; Xu, D. Flexural buckling of welded austenitic and duplex stainless steel I-section columns. *J. Constr. Steel Res.* **2016**, *122*, 339–353. [[CrossRef](#)]
76. Delincé, M.; Jacques, P.J.; Pardoën, T. Separation of size-dependent strengthening contributions in fine-grained Dual Phase steels by nanoindentation. *Acta Mater.* **2006**, *54*, 3395–3404. [[CrossRef](#)]
77. Li, Y.; Zhang, S.; He, Y.; Zhang, L.; Wang, L. Characteristics of the nitrated layer formed on AISI 304 austenitic stainless steel by high temperature nitriding assisted hollow cathode discharge. *Mater. Des.* **2014**, *64*, 527–534. [[CrossRef](#)]
78. Reyes-Hernández, D.; Manzano-Ramírez, A.; Encinas, A.; Sánchez-Cabrera, V.M.; de Jesús, Á.M.; García-García, R.; Orozco, G.; Olivares-Ramírez, J.M. Addition of nitrogen to GTAW welding duplex steel 2205 and its effect on fatigue strength and corrosion. *Fuel* **2017**, *198*, 165–169. [[CrossRef](#)]
79. Zhang, Z.; Zhang, H.; Zhao, H.; Li, J. Effect of prolonged thermal cycles on the pitting corrosion resistance of a newly developed LDX 2404 lean duplex stainless steel. *Corros. Sci.* **2016**, *103*, 189–195. [[CrossRef](#)]
80. Martins, M.; Casteletti, L.C. Heat treatment temperature influence on ASTM A890 GR 6A super duplex stainless steel microstructure. *Mater. Charact.* **2005**, *55*, 225–233. [[CrossRef](#)]
81. Vijayalakshmi, K.; Muthupandi, V.; Jayachitra, R. Influence of heat treatment on the microstructure, ultrasonic attenuation and hardness of SAF 2205 duplex stainless steel. *Mater. Sci. Eng. A* **2011**, *529*, 447–451. [[CrossRef](#)]
82. Ramkumar, K.D.; Mishra, D.; Vignesh, M.K.; Raj, B.G.; Arivazhagan, N.; Naren, S.V.; Kumar, S.S. Metallurgical and mechanical characterization of electron beam welded super-duplex stainless steel UNS 32750. *J. Manuf. Process.* **2014**, *16*, 527–534. [[CrossRef](#)]
83. Chen, C.Y.; Yen, H.W.; Yang, J.R. Sympathetic nucleation of austenite in a Fe-22Cr-5Ni duplex stainless steel. *Scr. Mater.* **2007**, *56*, 673–676. [[CrossRef](#)]
84. Park, C.J.; Rao, V.S.; Kwon, H.S. Effects of sigma phase on the initiation and propagation of pitting corrosion of duplex stainless steel. *Corrosion* **2005**, *61*, 76–83. [[CrossRef](#)]
85. Kordatos, J.D.; Fourlaris, G.; Papadimitriou, G. Effect of hydrogen and cooling rate on the mechanical and corrosion properties of SAF 2507 duplex stainless steel welds. *Mater. Sci. Forum.* **1999**, *318*, 615–620. [[CrossRef](#)]
86. Kobayashi, D.Y.; Wolyne, S. Evaluation of the low corrosion resistant phase formed during the sigma phase precipitation in duplex stainless steels. *Mater. Res.* **1999**, *2*, 239–247. [[CrossRef](#)]

87. Muthupandi, V.; Bala Srinivasan, P.; Seshadri, S.K.; Sundaresan, S. Effect of weld metal chemistry and heat input on the structure and properties of duplex stainless steel welds. *Mater. Sci. Eng. A* **2003**, *358*, 9–16. [[CrossRef](#)]
88. Selvabharathi, R.; Muralikannan, R. Influence of shot peening and plasma ion nitriding on tensile strength of 2205 duplex stainless steel using A-PAW. *Mater. Sci. Eng. A* **2018**, *709*, 232–240. [[CrossRef](#)]
89. Liu, H.; Jin, X. Electrochemical corrosion behavior of the laser continuous heat treatment welded joints of 2205 duplex stainless steel. *J. Wuhan Univ. Technol. Mater. Sci. Ed.* **2011**, *26*, 1140–1147. [[CrossRef](#)]
90. Zhang, Z.; Zhang, H.; Hu, J.; Qi, X.; Bian, Y.; Shen, A.; Xu, P.; Zhao, Y. Microstructure evolution and mechanical properties of briefly heat-treated SAF 2507 super duplex stainless steel welds. *Constr. Build. Mater.* **2018**, *168*, 338–345. [[CrossRef](#)]
91. Nikoosohbat, F.; Kheirandish, S.; Goodarzi, M.; Pouranvari, M. Effect of Tempering on the microstructure and mechanical properties of Resistance spot welded DP980 Dual Phase steel. *Mater. Technol.* **2015**, *49*, 133–138. [[CrossRef](#)]
92. Yang, Y.; Wang, Z.; Tan, H.; Hong, J.; Jiang, Y.; Jiang, L.; Li, J. Effect of a brief post-weld heat treatment on the microstructure evolution and pitting corrosion of laser beam welded UNS S31803 duplex stainless steel. *Corros. Sci.* **2012**, *65*, 472–480. [[CrossRef](#)]
93. Kuroda, T.; Ikeuchi, K.; Ikeda, H. Flash butt resistance welding for duplex stainless steels. *Vacuum* **2006**, *80*, 1331–1335. [[CrossRef](#)]
94. Wang, S.G.; Dong, G.P.; Ma, Q.H. Welding of duplex stainless steel composite plate: Influence on microstructural development. *Mater. Manuf. Process.* **2009**, *24*, 1383–1388. [[CrossRef](#)]
95. Korra, N.N.; Vasudevan, M.; Balasubramanian, K.R. Multi-objective optimization of activated tungsten inert gas welding of duplex stainless steel using response surface methodology. *Int. J. Adv. Manuf. Technol.* **2015**, *77*, 67–81. [[CrossRef](#)]
96. Mirakhorli, F.; Malek Ghaini, F.; Torkamany, M.J. Development of weld metal microstructures in pulsed laser welding of duplex stainless steel. *J. Mater. Eng. Perform.* **2012**, *21*, 2173–2176. [[CrossRef](#)]
97. Sun, X.; Stephens, E.V.; Khaleel, M.A. Effects of fusion zone size and failure mode on peak load and energy absorption of advanced high strength steel spot welds under lap shear loading conditions. *Eng. Fail. Anal.* **2008**, *15*, 356–367. [[CrossRef](#)]
98. Amana, B.; Singh Preet, M. Stress corrosion cracking of welded 2205 duplex stainless steel in sulfide-containing caustic solution. *J. Fail. Anal. Prev.* **2007**, *7*, 371–377. [[CrossRef](#)]
99. Luo, J.; Dong, Y.; Li, L.; Wang, X. Microstructure of 2205 duplex stainless steel joint in submerged arc welding by post weld heat treatment. *J. Manuf. Process.* **2014**, *16*, 144–148. [[CrossRef](#)]
100. Badji, R.; Bouabdallah, M.; Bacroix, B.; Kahloun, C.; Bettahar, K.; Kherrouba, N. Effect of solution treatment temperature on the precipitation kinetic of σ -phase in 2205 duplex stainless steel welds. *Mater. Sci. Eng. A* **2008**, *496*, 447–454. [[CrossRef](#)]
101. Sarlak, H.; Atapour, M.; Esmailzadeh, M. Corrosion behavior of friction stir welded lean duplex stainless steel. *Mater. Des.* **2015**, *66*, 209–216. [[CrossRef](#)]
102. Mourad, A.H.I.; Khourshid, A.; Sharef, T. Gas tungsten arc and laser beam welding processes effects on duplex stainless steel 2205 properties. *Mater. Sci. Eng. A* **2012**, *549*, 105–113. [[CrossRef](#)]
103. Yang, Y.; Yan, B.; Li, J.; Wang, J. The effect of large heat input on the microstructure and corrosion behaviour of simulated heat affected zone in 2205 duplex stainless steel. *Corros. Sci.* **2011**, *53*, 3756–3763. [[CrossRef](#)]
104. Sieurin, H.; Sandström, R. Austenite reformation in the heat-affected zone of duplex stainless steel 2205. *Mater. Sci. Eng. A* **2006**, *418*, 250–256. [[CrossRef](#)]
105. Verma, J.; Taiwade, R.V. Effect of welding processes and conditions on the microstructure, mechanical properties and corrosion resistance of duplex stainless steel weldments—A review. *J. Manuf. Process.* **2017**, *25*, 134–152. [[CrossRef](#)]
106. Tan, H.; Wang, Z.; Jiang, Y.; Yang, Y.; Deng, B.; Song, H.; Li, J. Influence of welding thermal cycles on microstructure and pitting corrosion resistance of 2304 duplex stainless steels. *Corros. Sci.* **2012**, *55*, 368–377. [[CrossRef](#)]
107. Young, M.C.; Tsay, L.W.; Shin, C.S.; Chan, S.L.I. The effect of short time post-weld heat treatment on the fatigue crack growth of 2205 duplex stainless steel welds. *Int. J. Fatigue.* **2007**, *29*, 2155–2162. [[CrossRef](#)]

108. Perren, R.A.; Suter, T.A.; Uggowitz, P.J.; Weber, L.; Magdowski, R.; Böhni, H.; Speidel, M.O. Corrosion resistance of super duplex stainless steels in chloride ion containing environments: Investigations by means of a new microelectrochemical method. I. Precipitation-free states. *Corros. Sci.* **2001**, *43*, 707–726. [[CrossRef](#)]
109. Malek Ghaini, F.; Hamed, M.J.; Torkamany, M.J.; Sabbaghzadeh, J. Weld metal microstructural characteristics in pulsed Nd: YAG laser welding. *Scr. Mater.* **2007**, *56*, 955–958. [[CrossRef](#)]
110. Saravanan, S.; Raghukandan, K.; Sivagurumanikandan, N. Pulsed Nd: YAG laser welding and subsequent post-weld heat treatment on super duplex stainless steel. *J. Manuf. Process.* **2017**, *25*, 284–289. [[CrossRef](#)]
111. Pramanik, A.; Littlefair, G.; Basak, A.K. Weldability of duplex stainless steel. *Mater. Manuf. Process.* **2015**, *30*, 1053–1068. [[CrossRef](#)]
112. Saravanan, S.; Raghukandan, K.; Sivagurumanikandan, N. Studies on metallurgical and mechanical properties of laser welded dissimilar grade steels. *J. Brazilian Soc. Mech. Sci. Eng.* **2017**, *39*, 3491–3498. [[CrossRef](#)]
113. Zou, Y.; Ueji, R.; Fujii, H. Mechanical properties of advanced active-TIG welded duplex stainless steel and ferrite steel. *Mater. Sci. Eng. A* **2015**, *620*, 140–148. [[CrossRef](#)]
114. Ramkumar, K.D.; Singh, A.; Raghuvanshi, S.; Bajpai, A.; Solanki, T.; Arivarasu, M.; Arivazhagan, N.; Narayanan, S. Metallurgical and mechanical characterization of dissimilar welds of austenitic stainless steel and super-duplex stainless steel—A comparative study. *J. Manuf. Process.* **2015**, *19*, 212–232. [[CrossRef](#)]
115. Jayalakshmi, M.; Huilgol, P.; Bhat, B.R.; Bhat, K.U. Microstructural characterization of low temperature plasma-nitrided 316L stainless steel surface with prior severe shot peening. *Mater. Des.* **2016**, *108*, 448–454. [[CrossRef](#)]
116. Richter, E.; Günzel, R.; Parasacandola, S.; Telbizova, T.; Kruse, O.; Möller, W. Nitriding of stainless steel and aluminium alloys by plasma immersion ion implantation. *Surf. Coatings Technol.* **2000**, *128–129*, 21–27. [[CrossRef](#)]
117. Olden, V.; Thaulow, C.; Johnsen, R. Modelling of hydrogen diffusion and hydrogen induced cracking in supermartensitic and duplex stainless steels. *Mater. Des.* **2008**, *29*, 1934–1948. [[CrossRef](#)]
118. Kvaale, P.E.; Olsen, S. Experience with Supermartensitic Stainless Steels in Flowline Applications. *Stainl. Steel Word* **1999**, *99*, 19–26.
119. Lippold, J.C.; Kotecki, D.J. *Martensitic Stainless Steel, Welding Metallurgy and Weldability Of Stainless Steels*, 1st ed.; Wiley: New York, NY, USA, 2005; pp. 58–60.
120. Muthusamy, C.; Karuppiyah, L.; Paulraj, S.; Kandasami, D.; Kandhasamy, R. Effect of heat input on mechanical and metallurgical properties of gas tungsten arc welded lean super martensitic stainless steel. *Mater. Res.* **2016**, *19*, 572–579. [[CrossRef](#)]
121. Köse, C.; Kaçar, R. The effect of preheat & post weld heat treatment on the laser weldability of AISI 420 martensitic stainless steel. *Mater. Des.* **2014**, *64*, 221–226. [[CrossRef](#)]
122. Schäfer, L. Influence of delta ferrite and dendritic carbides on the impact and tensile properties of a martensitic chromium steel. *J. Nucl. Mater.* **1998**, *258–263*, 1336–1339. [[CrossRef](#)]
123. Anderko, K.; Schäfer, L.; Materna-Morris, E. Effect of the δ -ferrite phase on the impact properties of martensitic chromium steels. *J. Nucl. Mater.* **1991**, *179–181*, 492–495. [[CrossRef](#)]
124. Baghjari, S.H.; Akbari Mousavi, S.A.A. Effects of pulsed Nd: YAG laser welding parameters and subsequent post-weld heat treatment on microstructure and hardness of AISI 420 stainless steel. *Mater. Des.* **2013**, *43*, 1–9. [[CrossRef](#)]
125. Bilmes, P.; Llorente, C.; Pérez Ipiña, J. Toughness and microstructure of 13Cr4NiMo high-strength steel welds. *J. Mater. Eng. Perform.* **2000**, *9*, 609–615. [[CrossRef](#)]
126. Kurt, B.; Orhan, N.; Somunkiran, I.; Kaya, M. The effect of austenitic interface layer on microstructure of AISI 420 martensitic stainless steel joined by keyhole PTA welding process. *Mater. Des.* **2009**, *30*, 661–664. [[CrossRef](#)]
127. Taneike, M.; Sawada, K.; Abe, F. Effect of carbon concentration on precipitation behavior of M23C6 carbides and MX carbonitrides in martensitic 9Cr steel during heat treatment. *Metall. Mater. Trans. A Phys. Metall. Mater. Sci.* **2004**, *35*, 1255–1262. [[CrossRef](#)]
128. Das, C.R.; Albert, S.K.; Sam, S.; Mastanaiah, P.; Chaitanya, G.M.S.K.; Bhaduri, A.K.; Jayakumar, T.; Murthy, C.V.S.; Kumar, E.R. Mechanical properties of 9Cr-1W reduced activation ferritic martensitic steel weldment prepared by electron beam welding process. *Fusion Eng. Des.* **2014**, *89*, 2672–2678. [[CrossRef](#)]
129. Berretta, J.R.; de Rossi, W.; David Martins das Neves, M.; Alves de Almeida, I.; Dias Vieira Junior, N. Pulsed Nd:YAG laser welding of AISI 304 to AISI 420 stainless steels. *Opt. Lasers Eng.* **2007**, *45*, 960–966. [[CrossRef](#)]

130. Khan, M.M.A.; Romoli, L.; Ishak, R.; Fiaschi, M.; Dini, G.; De Sanctis, M. Experimental investigation on seam geometry, microstructure evolution and microhardness profile of laser welded martensitic stainless steels. *Opt. Laser Technol.* **2012**, *44*, 1611–1619. [[CrossRef](#)]
131. Khan, M.M.A.; Romoli, L.; Fiaschi, M.; Sarri, F.; Dini, G. Experimental investigation on laser beam welding of martensitic stainless steels in a constrained overlap joint configuration. *J. Mater. Process. Technol.* **2010**, *210*, 1340–1353. [[CrossRef](#)]
132. Tavares, S.S.M.; Rodrigues, C.R.; Pardal, J.M.; Da Silva Barbosa, E.; De Abreu, H.F.G. Effects of post weld heat treatments on the microstructure and mechanical properties of dissimilar weld of supermartensitic stainless steel. *Mater. Res.* **2014**, *17*, 1336–1343. [[CrossRef](#)]
133. Zappa, S.; Svoboda, H.; Surian, E. Effect of Post-weld Heat Treatment on the Mechanical Properties of Supermartensitic Stainless Steel Deposit. *J. Mater. Eng. Perform.* **2017**, *26*, 514–521. [[CrossRef](#)]
134. Kumar, S.; Chaudhari, G.P.; Nath, S.K.; Basu, B. Effect of preheat temperature on weldability of martensitic stainless steel. *Mater. Manuf. Process.* **2012**, *27*, 1382–1386. [[CrossRef](#)]
135. Manugula, V.L.; Rajulapati, K.V.; Reddy, G.M.; Rao, K.B.S. Role of evolving microstructure on the mechanical properties of electron beam welded ferritic-martensitic steel in the as-welded and post weld heat-treated states. *Mater. Sci. Eng. A* **2017**, *698*, 36–45. [[CrossRef](#)]
136. Li, X.; Chen, J.; Hua, P.; Chen, K.; Kong, W.; Chu, H.; Wu, Y.; Zhou, W. Effect of post weld heat treatment on the microstructure and properties of Laser-TIG hybrid welded joints for CLAM steel. *Fusion Eng. Des.* **2018**, *128*, 177–181. [[CrossRef](#)]
137. Reddy, G.M.; Rao, V.V.; Raju, A.V.S. The effect of post-weld heat treatments on the microstructure and mechanical properties of maraging steel laser weldments. *Proc. Inst. Mech. Eng. Part L J. Mater. Des. Appl.* **2009**, *223*, 149–159. [[CrossRef](#)]
138. Sundaresan, S.; Manirajan, M.; Nageswara Rao, B. On the fracture toughness evaluation in weldments of a maraging steel rocket motor case. *Mater. Des.* **2010**, *31*, 4921–4926. [[CrossRef](#)]
139. An, J.; Meng, F.; Lv, X.; Liu, H.; Gao, X.; Wang, Y.; Lu, Y. Improvement of mechanical properties of stainless maraging steel laser weldments by post-weld ageing treatments. *Mater. Des.* **2012**, *40*, 276–284. [[CrossRef](#)]
140. Sarkari Khorrami, M.; Mostafaei, M.A.; Pouraliakbar, H.; Kokabi, A.H. Study on microstructure and mechanical characteristics of low-carbon steel and ferritic stainless steel joints. *Mater. Sci. Eng. A* **2014**, *608*, 35–45. [[CrossRef](#)]
141. Cho, H.H.; Han, H.N.; Hong, S.T.; Park, J.H.; Kwon, Y.J.; Kim, S.H.; Steel, R.J. Microstructural analysis of friction stir welded ferritic stainless steel. *Mater. Sci. Eng. A* **2011**, *528*, 2889–2894. [[CrossRef](#)]
142. Elangovan, S.; Balagopal, S.; Timper, M.; Bay, I.; Larsen, D.; Hartvigsen, J. Evaluation of ferritic stainless steel for use as metal interconnects for solid oxide fuel cells. *J. Mater. Eng. Perform.* **2004**, *13*, 265–273. [[CrossRef](#)]
143. Alizadeh-Sh, M.; Marashi, S.P.H.; Pouranvari, M. Resistance spot welding of AISI 430 ferritic stainless steel: Phase transformations and mechanical properties. *Mater. Des.* **2014**, *56*, 258–263. [[CrossRef](#)]
144. Venkata Ramana, P.; Madhusudhan Reddy, G.; Mohandas, T.; Gupta, A.V. Microstructure and residual stress distribution of similar and dissimilar electron beam welds - Maraging steel to medium alloy medium carbon steel. *Mater. Des.* **2010**, *31*, 749–760. [[CrossRef](#)]
145. Dewan, M.W.; Liang, J.; Wahab, M.A.; Okeil, A.M. Effect of post-weld heat treatment and electrolytic plasma processing on tungsten inert gas welded AISI 4140 alloy steel. *Mater. Des.* **2014**, *54*, 6–13. [[CrossRef](#)]
146. Abdullah, A.; Malaki, M.; Eskandari, A. Strength enhancement of the welded structures by ultrasonic peening. *Mater. Des.* **2012**, *38*, 7–18. [[CrossRef](#)]
147. Prasad Rao, K.; Janaki Ram, G.D.; Stucker, B.E. Improvement in corrosion resistance of friction stir welded aluminum alloys with micro arc oxidation coatings. *Scr. Mater.* **2008**, *58*, 998–1001. [[CrossRef](#)]
148. Jahazi, M.; Egbali, B. The influence of hot rolling parameters on the micro structure and mechanical properties of an ultra-high strength steel. *J. Mater. Process. Technol.* **2000**, *103*, 276–279. [[CrossRef](#)]
149. Ahmed, S.R.; Agarwal, L.A.; Daniel, B.S.S. Effect of Different Post Weld Heat Treatments on the Mechanical properties of Cr-Mo Boiler Steel Welded with SMAW Process. *Mater. Today Proc.* **2015**, *2*, 1059–1066. [[CrossRef](#)]
150. Dey, H.C.; Albert, S.K.; Bhaduri, A.K.; Roy, G.G.; Balakrishnan, R.; Panneerselvi, S. Effect of post-weld heat treatment (PWHT) time and multiple PWHT on mechanical properties of multi-pass TIG weld joints of modified 9Cr-1Mo steel. *Weld. World.* **2014**, *58*, 389–395. [[CrossRef](#)]

151. Taniguchi, G.; Yamashita, K. Effects of Post Weld Heat Treatment (PWHT) Temperature on Mechanical Properties of Weld Metals for High-Cr. *Kobelco Technol. Rev.* **2013**, *32*, 33–39.
152. Liang, J.; Wang, K.Y.; Guo, S.M.; Wahab, M.A. Influence of electrolytic plasma process on corrosion property of peened 304 austenitic stainless steel. *Mater. Lett.* **2011**, *65*, 510–513. [[CrossRef](#)]
153. Kellogg, H.H. Anode Effect in Aqueous Electrolysis. *J. Electrochem. Soc.* **1950**, *97*, 133. [[CrossRef](#)]
154. Gupta, P.; Tenhundfeld, G.; Daigle, E.O.; Ryabkov, D. Electrolytic plasma technology: Science and engineering—An overview. *Surf. Coatings Technol.* **2007**, *201*, 8746–8760. [[CrossRef](#)]
155. Baltazar Hernandez, V.H.; Kuntz, M.L.; Khan, M.I.; Zhou, Y. Influence of microstructure and weld size on the mechanical behaviour of dissimilar AHSS resistance spot welds. *Sci. Technol. Weld. Join.* **2008**, *13*, 769–776. [[CrossRef](#)]
156. Mehta, K.P.; Badheka, V.J. A review on dissimilar friction stir welding of copper to aluminum: Process, properties, and variants. *Mater. Manuf. Process.* **2016**, *31*, 233–254. [[CrossRef](#)]
157. Kush, M. Advanced Joining and Welding Techniques: An Overview. In *Advanced Manufacturing Technologies: Material Forming, Machining and Tribology*; Gupta, K., Ed.; Springer: Cham, Switzerland, 2017; pp. 101–134. [[CrossRef](#)]
158. Mehta, K.P.; Badheka, V.J. Effects of tilt angle on the properties of dissimilar friction stir welding copper to aluminum. *Mater. Manuf. Process.* **2016**, *31*, 255–263. [[CrossRef](#)]
159. Padmanaban, G.; Balasubramanian, V. Optimization of laser beam welding process parameters to attain maximum tensile strength in AZ31B magnesium alloy. *Opt. Laser Technol.* **2010**, *42*, 1253–1260. [[CrossRef](#)]
160. Vieira, L.A.; Fernandes, F.B.; Miranda, R.M.; Silva, R.J.C.; Quintino, L.; Cuesta, A.; Ocaña, J.L. Mechanical behaviour of Nd:YAG laser welded superelastic NiTi. *Mater. Sci. Eng. A* **2011**, *528*, 5560–5565. [[CrossRef](#)]
161. Qiu, X.M.; Li, M.G.; Sun, D.Q.; Liu, W.H. Study on brazing of TiNi shape memory alloy with stainless steels. *J. Mater. Process. Technol.* **2006**, *176*, 8–12. [[CrossRef](#)]
162. Liu, P.; Shi, Q.; Wang, W.; Wang, X.; Zhang, Z. Microstructure and XRD analysis of FSW joints for copper T2/aluminium 5A06 dissimilar materials. *Mater. Lett.* **2008**, *62*, 4106–4108. [[CrossRef](#)]
163. Tsujino, J.; Hidai, K.; Hasegawa, A.; Kanai, R.; Matsuura, H.; Matsushima, K.; Ueoka, T. Ultrasonic butt welding of aluminum, aluminum alloy and stainless steel plate specimens. *Ultrasonics* **2002**, *40*, 371–374. [[CrossRef](#)]
164. Madhusudhan Reddy, G.; Sambasiva Rao, A.; Mohandas, T. Role of electroplated interlayer in continuous drive friction welding of AA6061 to AISI 304 dissimilar metals. *Sci. Technol. Weld. Join.* **2008**, *13*, 619–628. [[CrossRef](#)]
165. Sadeghi, B.; Sharifi, H.; Rafiei, M.; Tayebi, M. Effects of post weld heat treatment on residual stress and mechanical properties of GTAW: The case of joining A537CL1 pressure vessel steel and A321 austenitic stainless steel. *Eng. Fail. Anal.* **2018**, *94*, 396–406. [[CrossRef](#)]
166. Sawada, Y.K.; Nakamura, M. Lapped friction stir welding between ductile cast irons and stainless steels. *Weld. Int.* **2013**, *27*, 121–128. [[CrossRef](#)]
167. Kolukisa, S. The effect of the welding temperature on the weldability in diffusion welding of martensitic (AISI 420) stainless steel with ductile (spheroidal graphite-nodular) cast iron. *J. Mater. Process. Technol.* **2007**, *186*, 33–36. [[CrossRef](#)]
168. Nekouie Esfahani, M.R.; Coupland, J.; Marimuthu, S. Microstructural and mechanical characterisation of laser-welded high-carbon and stainless steel. *Int. J. Adv. Manuf. Technol.* **2015**, *80*, 1449–1456. [[CrossRef](#)]
169. Kim, S.; Lee, S.; Han, K.; Hong, S.; Lee, C. Cracking behavior in a dissimilar weld between high silicon nodular cast iron and ferritic stainless steel. *Met. Mater. Int.* **2010**, *16*, 483–488. [[CrossRef](#)]
170. Fraš, E.; López, H.F. A theoretical analysis of the chilling susceptibility of hypoeutectic FeC alloys. *Acta Metall. Mater.* **1993**, *41*, 3575–3583. [[CrossRef](#)]
171. Riposan, I.; Chisamera, M.; Stan, S.; White, D. Chilling properties of Ba/Ca/Sr inoculated grey cast irons. *Int. J. Cast Met. Res.* **2007**, *20*, 90–97. [[CrossRef](#)]
172. Vach, M.; Kunikova, T.; Domankova, M.; Ševc, P.; Čaplovič, L.; Gogola, P.; Janovec, J. Evolution of secondary phases in austenitic stainless steels during long-term exposures at 600, 650 and 800 C. *Mater. Charact.* **2008**, *59*, 1792–1798. [[CrossRef](#)]
173. Taban, E.; Kaluc, E.; Dhooge, A. Hybrid (plasma + gas tungsten arc) weldability of modified 12% Cr ferritic stainless steel. *Mater. Des.* **2009**, *30*, 4236–4242. [[CrossRef](#)]

174. Curiel, F.F.; García, R.; López, V.H.; González-Sánchez, J. Effect of magnetic field applied during gas metal arc welding on the resistance to localised corrosion of the heat affected zone in AISI 304 stainless steel. *Corros. Sci.* **2011**, *53*, 2393–2399. [[CrossRef](#)]
175. Amuda, M.O.H.; Mridha, S. Grain refinement in ferritic stainless steel welds: The journey so far. *Adv. Mater. Res.* **2010**, *83–86*, 1165–1172. [[CrossRef](#)]
176. Sathiya, P.; Aravindan, S.; Haq, A.N. Some experimental investigations on friction welded stainless steel joints. *Mater. Des.* **2008**, *29*, 1099–1109. [[CrossRef](#)]
177. Kumar, S.; Shahi, A.S. Effect of heat input on the microstructure and mechanical properties of gas tungsten arc welded AISI 304 stainless steel joints. *Mater. Des.* **2011**, *32*, 3617–3623. [[CrossRef](#)]
178. Dadfar, M.; Fathi, M.H.; Karimzadeh, F.; Dadfar, M.R.; Saatchi, A. Effect of TIG welding on corrosion behavior of 316L stainless steel. *Mater. Lett.* **2007**, *61*, 2343–2346. [[CrossRef](#)]
179. Ghorbani, S.; Ghasemi, R.; Ebrahimi-Kahrizsangi, R.; Hojjati-Najafabadi, A. Effect of post weld heat treatment (PWHT) on the microstructure, mechanical properties, and corrosion resistance of dissimilar stainless steels. *Mater. Sci. Eng. A* **2017**, *688*, 470–479. [[CrossRef](#)]
180. Zhang, J.; Huang, B.; Wu, Q.; Li, C.; Huang, Q. Effect of post-weld heat treatment on the mechanical properties of CLAM/316L dissimilar joint. *Fusion Eng. Des.* **2015**, *100*, 334–339. [[CrossRef](#)]
181. Sun, L.; Huang, W.M.; Ding, Z.; Zhao, Y.; Wang, C.C.; Purnawali, H.; Tang, C. Stimulus-responsive shape memory materials: A review. *Mater. Des.* **2012**, *33*, 577–640. [[CrossRef](#)]
182. Sadrnezhaad, S.K.; Nemati, N.H.; Bagheri, R. Improved adhesion of NiTi wire to silicone matrix for smart composite medical applications. *Mater. Des.* **2009**, *30*, 3667–3672. [[CrossRef](#)]
183. Stolyarov, V.V. Deformability and nanostructuring of TiNi shape-memory alloys during electroplastic rolling. *Mater. Sci. Eng. A* **2009**, *503*, 18–20. [[CrossRef](#)]
184. Oliveira, J.P.; Duarte, J.F.; Inácio, P.; Schell, N.; Miranda, R.M.; Santos, T.G. Production of Al/NiTi composites by friction stir welding assisted by electrical current. *Mater. Des.* **2017**, *113*, 311–318. [[CrossRef](#)]
185. Prabu, S.M.; Madhu, H.C.; Perugu, C.S.; Akash, K.; Mithun, R.; Kumar, P.A.; Kailas, S.V.; Anbarasu, M.; Palani, I.A. Shape memory effect, temperature distribution and mechanical properties of friction stir welded nitinol. *J. Alloys Compd.* **2019**, *776*, 334–345. [[CrossRef](#)]
186. Novák, P.; Mejzliková, L.; Michalčová, A.; Čapek, J.; Beran, P.; Vojtěch, D. Effect of SHS conditions on microstructure of NiTi shape memory alloy. *Intermetallics* **2013**, *42*, 85–91. [[CrossRef](#)]
187. Greger, M.; Kander, L.; Snasel, V.; Cerny, M. Microstructure evolution of pure titanium during ECAP. *Mater. Des.* **2011**, *18*, 97–104.
188. Mehrpouya, M.; Gisario, A.; Elahinia, M. Laser welding of NiTi shape memory alloy: A review. *J. Manuf. Process.* **2018**, *31*, 162–186. [[CrossRef](#)]
189. Li, H.; Sun, D.; Cai, X.; Dong, P.; Gu, X. Laser welding of TiNi shape memory alloy and stainless steel using Co filler metal. *Opt. Laser Technol.* **2013**, *45*, 453–460. [[CrossRef](#)]
190. Chen, Y.; Sun, S.; Zhang, T.; Zhou, X.; Li, S. Effects of post-weld heat treatment on the microstructure and mechanical properties of laser-welded NiTi/304SS joint with Ni filler. *Mater. Sci. Eng. A* **2020**, *771*, 138545. [[CrossRef](#)]
191. Mirshekari, G.R.; Saatchi, A.; Kermanpur, A.; Sadrnezhaad, S.K. Effect of Post Weld Heat Treatment on Mechanical and Corrosion Behaviors of NiTi and Stainless Steel Laser-Welded Wires. *J. Mater. Eng. Perform.* **2016**, *25*, 2395–2402. [[CrossRef](#)]
192. Chiu, K.Y.; Cheng, F.T.; Man, H.C. Corrosion behavior of AISI 316L stainless steel surface-modified with NiTi. *Surf. Coatings Technol.* **2006**, *200*, 6054–6061. [[CrossRef](#)]
193. Groza, J.R.; Eslamloo-Grami, M.; Bandy, R. The effect of thermo-mechanical treatment on The pitting corrosion of reinforcing carbon steel bars. *Mater. Corros.* **1993**, *44*, 359–366. [[CrossRef](#)]
194. Akbarimousavi, S.A.A.; GohariKia, M. Investigations on the mechanical properties and microstructure of dissimilar cp-titanium and AISI 316L austenitic stainless steel continuous friction welds. *Mater. Des.* **2011**, *32*, 3066–3075. [[CrossRef](#)]
195. Fuji, A.; North, T.H.; Ameyama, K.; Futamata, M. Improving tensile strength and bend ductility of titanium/AISI 304L stainless steel friction welds. *Mater. Sci. Technol.* **1992**, *8*, 219–235. [[CrossRef](#)]
196. Fuji, A.; Ameyama, K.; North, T.H. Improved mechanical properties in dissimilar Ti-AISI 304L joints. *J. Mater. Sci.* **1996**, *31*, 819–827. [[CrossRef](#)]

197. Merola, M.; Escourbiac, F.; Raffray, R.; Chappuis, P.; Hirai, T.; Martin, A. Overview and status of ITER internal components. *Fusion Eng. Des.* **2014**, *89*, 890–895. [[CrossRef](#)]
198. Barceloux, D.G.; Barceloux, D. Copper. *Clin. Toxicol.* **1999**, *37*, 217–230. [[CrossRef](#)] [[PubMed](#)]
199. Yu, J.; Wang, G.; Rong, Y. Experimental Study on the Surface Integrity and Chip Formation in the Micro Cutting Process. *Procedia Manuf.* **2015**, *1*, 655–662. [[CrossRef](#)]
200. Mohammed, M.N.; Omar, M.Z.; Salleh, M.S.; Alhawari, K.S.; Kapranos, P. Semisolid Metal Processing Techniques for Nondendritic Feedstock Production. *Sci. World, J.* **2013**, *2013*, 752175. [[CrossRef](#)]
201. Weigl, M.; Schmidt, M. Influence of the feed rate and the lateral beam displacement on the joining quality of laser-welded copper-stainless steel connections. *Phys. Procedia.* **2010**, *5*, 53–59. [[CrossRef](#)]
202. Budkin, Y.V. Welding joints in dissimilar metals. *Weld. Int.* **2011**, *25*, 523–525. [[CrossRef](#)]
203. Uzun, H.; Dalle Donne, C.; Argagnotto, A.; Ghidini, T.; Gambaro, C. Friction stir welding of dissimilar Al 6013-T4 To X5CrNi18-10 stainless steel. *Mater. Des.* **2005**, *26*, 41–46. [[CrossRef](#)]
204. Lee, W.B.; Schmuecker, M.; Mercardo, U.A.; Biallas, G.; Jung, S.B. Interfacial reaction in steel-aluminum joints made by friction stir welding. *Scr. Mater.* **2006**, *55*, 355–358. [[CrossRef](#)]
205. Tanaka, T.; Morishige, T.; Hirata, T. Comprehensive analysis of joint strength for dissimilar friction stir welds of mild steel to aluminum alloys. *Scr. Mater.* **2009**, *61*, 756–759. [[CrossRef](#)]
206. Song, J.L.; Lin, S.B.; Yang, C.L.; Fan, C.L. Effects of Si additions on intermetallic compound layer of aluminum-steel TIG welding-brazing joint. *J. Alloys Compd.* **2009**, *488*, 217–222. [[CrossRef](#)]
207. Dharmendra, C.; Rao, K.P.; Wilden, J.; Reich, S. Study on laser welding-brazing of zinc coated steel to aluminum alloy with a zinc based filler. *Mater. Sci. Eng. A* **2011**, *528*, 1497–1503. [[CrossRef](#)]
208. Bang, H.; Bang, H.; Kim, H.; Kim, J.; Oh, I.; Ro, C. A Study on the weldability and mechanical characteristics of dissimilar materials butt joints by laser assisted friction stir welding. *J. Weld. Join.* **2010**, *28*, 70–75. [[CrossRef](#)]
209. Echaabi, J.; Nziengui, M.B.; Hattabi, M. Compressibility and relaxation models for fibrous reinforcements in Liquid Composite Moulding. *Int. J. Mater. Form.* **2008**, *1*, 185–188. [[CrossRef](#)]
210. Joshi, G.R.; Badheka, V.J. Microstructures and Properties of Copper to Stainless Steel Joints by Hybrid FSW. *Metallogr. Microstruct. Anal.* **2017**, *6*, 470–480. [[CrossRef](#)]
211. Mofid, M.A.; Abdollah-zadeh, A.; Malek Ghaini, F. The effect of water cooling during dissimilar friction stir welding of Al alloy to Mg alloy. *Mater. Des.* **2012**, *36*, 161–167. [[CrossRef](#)]
212. Zhang, J.; Shen, Y.; Yao, X.; Xu, H.; Li, B. Investigation on dissimilar underwater friction stir lap welding of 6061-T6 aluminum alloy to pure copper. *Mater. Des.* **2014**, *64*, 74–80. [[CrossRef](#)]
213. Bang, H.S.; Bang, H.S.; Jeon, G.H.; Oh, I.H.; Ro, C.S. Gas tungsten arc welding assisted hybrid friction stir welding of dissimilar materials Al6061-T6 aluminum alloy and STS304 stainless steel. *Mater. Des.* **2012**, *37*, 48–55. [[CrossRef](#)]
214. Dong, H.; Liao, C.; Yang, L.; Dong, C. Effects of post-weld heat treatment on dissimilar metal joint between aluminum alloy and stainless steel. *Mater. Sci. Eng. A* **2012**, *550*, 423–428. [[CrossRef](#)]

